Faunal and environmental drivers of carbon and nitrogen cycling along a permeability gradient in shallow North Sea sediments

Elise Toussaint [a,b,*,1], Emil De Borger [a,c,e,1], Ulrike Braeckman [a], Annelies De Backer [d], Karline Soetaert [a,c,e], Jan Vanaverbeke [a,b]

[a] Ghent University, Department of Biology, Marine Biology Research Group, Krijgslaan 281/S8, 9000 Ghent, Belgium
[b] Royal Belgian Institute of Natural Sciences, Operational Directorate Natural Environment, Marine Ecology and Management, Rue Vautier 29, 1000 Brussels, Belgium
[c] Royal Netherlands Institute of Sea Research (NIOZ), Department of Estuarine and Delta Systems, Korringaweg 7, P.O. Box 140, 4401, NT, Yerseke, the Netherlands
[d] Flanders Research Institute for Agriculture, Fisheries and Food (ILVO), Aquatic Environment and Quality, Ankerstraat 1, 8400 Oostende, Belgium
[e] Utrecht University, Heidelberglaan 8, 3584, CS, Utrecht, the Netherlands

HIGHLIGHTS

- Strong correlation between sediment properties, fauna and biogeochemical cycling.
- Benthic oxic mineralization and nitrification mainly regulated by faunal activities.
- Benthic anoxic mineralization mainly regulated by sediment properties.
- Macrofaunal activities have variable effects across habitats.
- Regression models are a useful tool to predict/understand the impact of human activities.

GRAPHICAL ABSTRACT
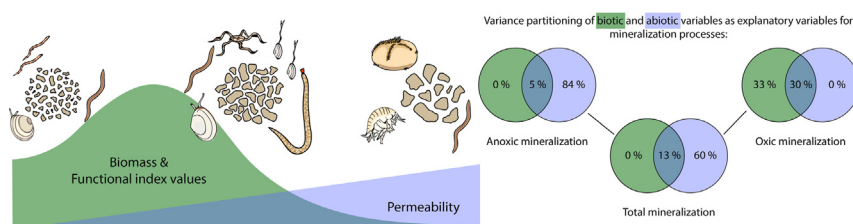
ARTICLE INFO

ABSTRACT

Ecosystem functions are driven by abiotic and biotic factors, but due to high collinearity of both, it is often difficult to disentangle the drivers of these ecosystem functions. We studied sedimentological and faunal controls of benthic organic matter mineralization, a crucial ecosystem process provided for by sediments of shelf seas. Subtidal benthic habitats representative of the wide permeability gradient found in the Belgian Part of the North Sea (Northeast Atlantic Shelf) were characterized in terms of sediment descriptors, macrofauna, and sediment biogeochemistry was estimated. Our results confirmed a strong correlation between sediment characteristics and macrofauna, and estimated sediment biogeochemical process rates were clearly linked to both. Results of variance partitioning and statistical modelling showed that oxic mineralization and nitrification were mainly regulated by faunal activities whereas anoxic mineralization was regulated by sediment properties, with permeability as a decisive factor. Both biotic and abiotic factors were needed to explain variability in oxygen consumption and total mineralization estimates, suggesting that macrofaunal activities have different effects across habitats. The statistical models were a useful tool to interpret the impact of anthropogenic activities in the study area and represent a step towards predicting the effects of human activities on crucial ecosystem functions.

© 2021 Elsevier B.V. All rights reserved.

* Corresponding author at: Ghent University, Department of Biology, Marine Biology Research Group, Krijgslaan 281/S8, 9000 Ghent, Belgium.
E-mail address: etoussaint@naturalsciences.be (E. Toussaint).
[1] Shared first authorship.

1. Introduction

It is well accepted that ecosystem functions, i.e. changes in energy and matter over time and space through biological activity (Snelgrove

et al., 2014), are driven by biodiversity interacting with abiotic and anthropogenic drivers (Duncan et al., 2015). Species assemblages, in turn, are shaped by adaptations to the prevailing environmental conditions in their habitat (Díaz and Cabido, 2001; Violle et al., 2007), the so-called functional response traits (Lavorel and Garnier, 2002). At the same time, species are characterized by a set of functional effect traits, having a direct or indirect role in ecosystem functioning (Lavorel and Garnier, 2002). This spatial pairing of species functional response and effect traits often generates a strong collinearity, which makes it difficult to disentangle the relative importance of biotic and abiotic drivers of ecosystem functions (Godbold and Solan, 2009).

In marine sediments, the mineralization of organic matter to free nutrients is an important ecosystem process, as this recycling mechanism drives biogeochemical cycling, which supports primary production in the water column (Soetaert and Middelburg, 2009; Provoost et al., 2013) and many important element cycles (Jørgensen, 2000). Typically, organic matter mineralization occurs through various processes, which are regulated by organic matter concentrations, the availability of oxygen (oxic vs. anoxic mineralization), and other electron acceptors such as nitrate (denitrification), metal oxides, and sulphate (Froelich et al., 1979). Shelf seas are especially important as they account for up to 80% of global carbon mineralization, despite covering only 7% of the marine surface (Wollast, 1998). Organic matter mineralization and other ecosystem functions are the result of the functional effect of the organisms present, and habitat structuring forces such as hydrodynamics, and the natural and anthropogenic disturbance regime. The highly dynamic nature of coastal areas, combined with the high degree of anthropogenic disturbances (Eigaard et al., 2017; Fettweis et al., 2009; Van De Velde et al., 2018), leads to a heterogeneous patchwork of habitats with strongly differing mineralization regimes, despite occurring in close proximity to one another (Braeckman et al., 2014; Neumann et al., 2017; Gogina et al., 2018).

Local sediment characteristics such as grain size distribution, permeability (the capacity to transmit fluid), and porosity (the water content), influence the redox zonation patterns in which microbially mediated mineralization processes occur (Böttcher et al., 2000; Llobet-Brossa et al., 2002; Probandt et al., 2017), by providing binding sites for organic matter (Mayer, 1994) and by regulating the exchange of oxygen, organic matter, and other reactants between the sediment and the overlying water (De Beer et al., 2005; Huettel et al., 2014). Large, connected pore-spaces in coarse grained, permeable sediments allow for advective flows, resulting in high organic matter turnover rates fuelled by a high oxygen supply (Huettel and Rusch, 2000; Ehrenhauss et al., 2004). In contrast, cohesive sediments are characterized by smaller and less connected interstitial spaces, so that diffusive processes, molecular diffusion or local transport stimulated by benthic fauna, dominate solute and particle transport (Aller, 1980; Gust and Harrison, 1981; Aller and Yingst, 1985; Aller and Aller, 1992; Huettel and Gust, 1992).

Organic matter mineralization processes are also affected by the fauna inhabiting this sediment gradient. Bioturbation, the faunal behaviour that results in particle displacement and increased exchange of solutes across the sediment-water interface (Aller and Yingst, 1985; Matisoff et al., 1985; Kristensen et al., 2012; Gogina et al., 2018), affects the vertical and horizontal distribution of organic matter, oxygen, and other electron acceptors involved in the mineralization processes (Kristensen, 2001; Na et al., 2008; Tous Rius et al., 2018). Functional indices such as the bioturbation potential of the community (BP_c) (Solan et al., 2004) and the irrigation potential of the community (IP_c) (Wrede et al., 2018), have been developed to approximate faunal activities, respectively particle mixing and ventilation, using functional effect traits. Recently, those functional indices have been applied to relate benthic communities to benthic ecosystem processes (Van Colen et al., 2012; Braeckman et al., 2014; Wrede et al., 2019; De Borger et al., 2020).

Benthic communities are closely linked to specific habitat types because of adaptations to hydrodynamic conditions, and sedimentological variables (Van Hoey et al., 2004; Degraer et al., 2008). As a result, the expression of functional effect traits affecting ecosystem functions, such as biological particle mixing (bio-mixing), or burrow ventilation is inherently coupled to the habitat in which the species occur (Snelgrove and Butman, 1994; Bremner et al., 2003; Breine et al., 2018).

Empirical information on how fauna and the physical environment drive ecosystem functions across environmental settings is needed to improve our understanding of coastal marine ecosystems and to evaluate how the quantity and quality of the delivery of ecosystem services, and the benefits that humans obtain from ecosystems, could be affected in scenarios of future change (Snelgrove et al., 2014; Hillman et al., 2020).

To quantify the degree to which faunal activities and the physico-chemical sediment characteristics influence specific mineralization processes, we investigated the sediment biogeochemistry and associated physico-chemical and biological characteristics, in contrasting environments in the Belgian Part of the North Sea (BPNS). This is a shallow coastal region where a wide gradient of permeable to cohesive sediments is found in close proximity (Braeckman et al., 2014), and where the distribution of benthic communities has been mapped extensively (Van Hoey et al., 2004; Degraer et al., 2008; Breine et al., 2018). More so, the small size of the BPNS (3462 km^2) ensures that temperature variations, light regime, and the magnitude of the phytoplankton bloom are relatively uniform throughout the study area (Rousseau et al., 2006).

Specific aims in the presented research were (1) to determine which mineralization processes are influenced predominantly by the abiotic components and which ones by the biotic components, and (2) to investigate which descriptor of the faunal activities (BP_c or IP_c) is most suited as a predictor of individual biogeochemical processes: oxic mineralization, nitrogen mineralization (including nitrification, denitrification, and dissimilatory nitrate reduction or DNRA), and anoxic mineralization (investigated as the collection of individual anoxic processes). Our hypothesis was that oxic mineralization processes would be more associated with biological features of the environment, most specifically with aspects of burrow ventilation, whereas anoxic mineralization processes would be stronger related to physical aspects of the sediment.

2. Materials and methods

2.1. Field sampling

In September 2016 and 2017, sediment, water column and benthic communities were sampled along a gradient of sediment permeability in the Belgian Part of the North Sea on board of *RV* Simon Stevin. Samples were collected at 5 stations (St. 130, St. 780, St. BRN11, St. 330, St. BBEG) in 2016 and at 7 stations (St. 130, St. 780, St. 120, St. BRN11, St. D6N, St. 330, St. D6S) in 2017 (Fig. 1, Appendix A in supplementary material). Amongst those stations, some are heavily impacted by human activities: BRN11 is located in a former aggregate extraction site that is abandoned since January 2015; BBEG is located in close proximity to an offshore wind farm under construction, and D6N and D6S are located 200 m north and south respectively from a wind turbine in the C-Power wind farm, operational since 2008 (Coates et al., 2014). All samples were collected at the end of summer to target the period with the highest benthic mineralization rates in the study area (Provoost et al., 2013; Braeckman et al., 2014).

At each station, a CTD-cast was performed to determine bottom water temperature. Bottom water ($\pm$ 1 m above the seafloor) was sampled with a 5 L NISKIN bottle to determine nutrient concentrations. Additional NISKIN bottles were closed at depth to collect bottom water used during incubation experiments. This water was stored in sealed vats, until further use in the laboratory.

A NIOZ box corer (0.028 m^2) was deployed three times at each station to collect undisturbed sediments, from which three subsamples were taken to characterize the sediment in terms of (1) permeability (plexiglass core, inner diameter, i.Ø: 3.6 cm; length: $\pm$25 cm), (2) granulometry and porosity (cut off syringe, upper 3 cm, 10 mL),
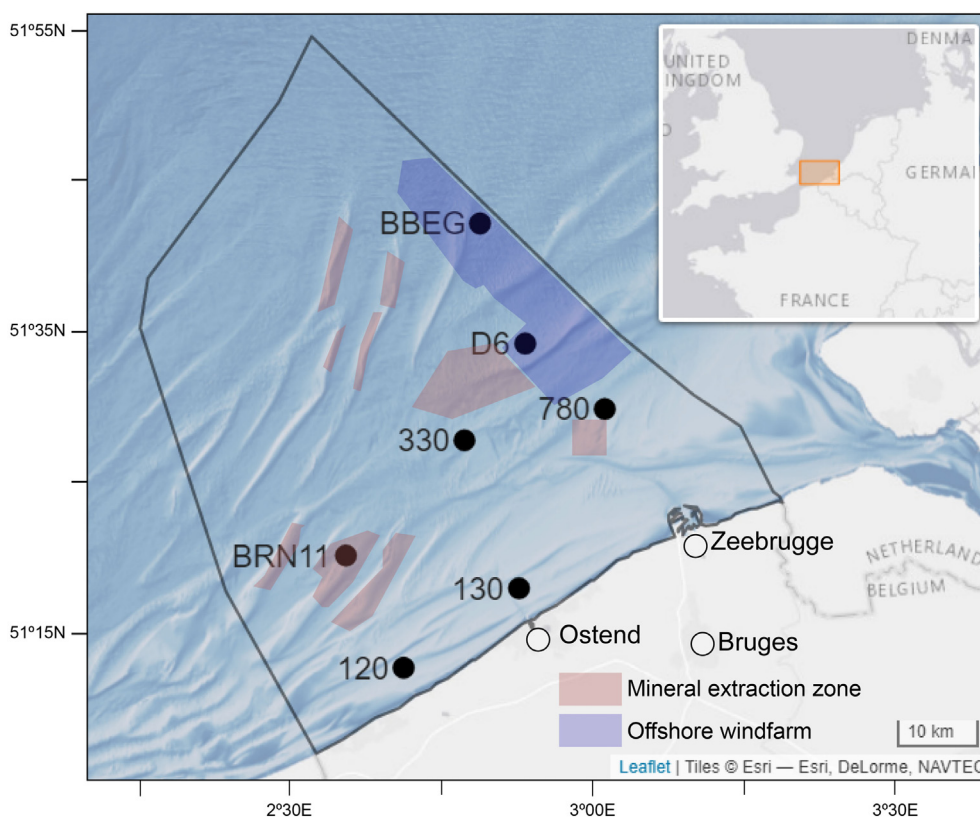
Fig. 1. Sampling sites (dots) in the Belgian Exclusive Economic Zone (EEZ, black outline) Basemap: © Esri, depth raster by (GEBCO Compilation Group, 2020), polygons by RBINS (MUMM Scientific Service, 2015).

and (3) pigments, total organic carbon, total nitrogen and total organic matter (TOC, TN and TOM) (cut off syringe, upper 3 cm, 5 mL). Porosity, TOC/TN and TOM samples were stored at −20 °C and pigments samples were stored in liquid nitrogen onboard and transferred to the −80 °C freezer in the lab.

Within each box core, one plexiglass core (cohesive sediment: i.Ø: 10 cm, height: 25 cm; permeable sediment: i.Ø: 19 cm to allow for advective porewater flow later, height: 30 cm) was inserted into the sediment to a depth of 10 to 15 cm, enclosing ±10 cm of overlying water. The cores were excavated from the box core, closed with a lid at the bottom, carefully filled up with in situ sea water without disturbing the sediment surface and placed in a tank of sea water at ambient temperature. Within 10 h, the cores were transported to a climate room set at 19.3 °C in the laboratory (in situ bottom water temperature for all stations was between 19 and 20 °C for both years, see Table A.1 Appendix A for incubation volumes, temperature, and salinity).

For the cohesive sediments, Teflon-coated magnet rings (~2.5 cm) were placed in the small cores, 5 cm above the sediment-water interface. A homogeneous mixing of the water column was ensured with a rotating central magnet. The rotation speed was kept below the resuspension rate and did not induce an advection flow in the sediment. For permeable sediment, the lids were equipped with a flat stirring disk which was placed at 5.4 cm above the sediment surface. The rotation speed was set at 40 rpm, allowing an advection porewater flow in the permeable sediment (Huettel and Rusch, 2000). With these settings, an advective porewater flow corresponding to the lower end of in situ conditions was simulated (Oldham et al., 2004; Van den Eynde, 2017). The overlying water was kept aerated until the start of the incubation. After 36 h of acclimatization in the temperature-controlled room, the overlying water in the cores was replaced by freshly oxygenated in situ sea water.

Bio-irrigation was measured following the decrease of a tracer in the water overlying the sediment in the experimental units (Glud et al.,

1996; De Smet et al., 2016; De Borger et al., 2020). In 2016, the overlying sea water was mixed with sodium bromide ($[NaBr]_{final} = 0.01$ mol L^{-1}) while in 2017, the newly replaced sea water was spiked with a uranine solution ($C_{20}H_{14}Na_2O_7$; $[uranine]_{final} = 10–15$ μg L^{-1}), a tracer that is cheaper and easier to analyse.

The cores were then sealed air-tight with lids equipped with gas-tight sampling ports and incubated in the dark. The incubations lasted for 2 to 8 h depending on the oxygen concentration in the overlying water which was not allowed to decrease below 50% of the initial saturation (see Section 2.2.2.1.). The overlying water was subsampled at the beginning (T_0) and at the end (T_{end}) of the incubation and, depending on the length of the incubation, at one (T_1) or two (T_2) moments in between. Using a glass syringe, subsamples were collected for O_2 (only in 2016: 1×10 mL), dissolved inorganic carbon (DIC) (2×6 mL), dissolved inorganic nitrogen (DIN – NO_x, NH_x) (2×10 mL) and the irrigation tracer (Br$^-$ or Uranine) (2×3 mL).

When a water sample was collected, the same volume of sea water collected from the field was simultaneously inserted into the core through the second sampling port to prevent aeration. This replacing sea water will be referred to as tank water. Subsamples of the tank water were taken at each sampling time for O_2, DIC, DIN, phosphate, silicate, and irrigation tracer. Sampling volumes were similar as described above. In total, 36 cores were incubated following this procedure; two of them were lost due to experimental errors.

DIC samples were transferred to Exetainers which were directly closed hermetically and fixed with mercury chloride ($HgCl_2$: 10 μL, 3%). DIC, bromide and uranine samples were stored at 4 °C until analysis. Nutrient samples were filtered through Whatman^{TM} GF/F filters and stored at −20 °C until further analysis.

After the incubation, the remaining sediment was sieved on a 1 mm mesh to collect the macrofauna, which was fixed on 70% ethanol until processing (following Gaston et al. (1996), Jørgensen et al. (2005), and Wetzel et al. (2005)).

2.2. Sample processing

2.2.1. Sediment parameters

Sediment grain size was determined by laser diffraction on freeze dried and sieved sediment samples in a Malvern Mastersizer 2000 (McCave et al., 1986). Grain size fractions were determined as volume percentages according to the Wentworth scale (Wentworth, 1922): clay/silt (<63 μm), very fine sand (vfines: 63–125 μm), fine sand (fines: 125–250 μm), medium sand (250–500 μm), and coarse sand (500 μm–1 mm). The median grain size (MGS) was calculated on the fraction <1 mm.

Water content (weight %) was determined as the volume of water removed by freeze drying wet sediment samples. Sediment porosity was determined from water content and solid phase density measurements (determined by measuring the mass of sediment needed to displace 1 mL of water), accounting for the salt content of the porewater.

The % of total organic matter (TOM) was calculated by weighing the sediment before and after burning (2 h at 500 °C) all organic material in dried (min 48 h at 60 °C) sediment.

The molar C/N ratio was calculated from the percentages of total organic carbon (TOC) and total N (TN), determined using an Interscience Flash 2000 organic element analyser (uncertainty: 0.01%, standard used: sulphanilamide). The permeability of sediment in the i.Ø 3.6 cm sampling cores was determined with a permeameter (Buchanan, 1984) in 2017. In 2016, sediment permeability was calculated after Hazen in Eggleston and Rojstaczer (1998) (Eq. (1)), using the first decile of the grain size distribution (d_{10}) and the kinematic viscosity (v):

$$Permeability = 1.1019 \cdot 10^3 m^{-2} s \cdot d\frac{2}{10} \cdot v \tag{1}$$

2.2.2. Solute concentrations and fluxes

2.2.2.1. Sediment community oxygen consumption (SCOC).
In 2016, the oxygen concentration of the water in the incubation cores was determined discretely by inserting an oxygen microsensor (Unisense, 100 μm tip, 2-point calibration) into a subsample of the overlying water. In 2017, the oxygen concentration was continuously monitored using a robust oxygen miniprobe (Firesting, 3 mm Ø, 10 cm long, 2-point calibration). In both sampling campaigns, SCOC was determined from the linear decrease of oxygen concentration in the overlying water between T_{end} and T_1, standardized for overlying water volume and fluid exchange surface and correcting for concentration changes due to the water replacement.

2.2.2.2. DIN and DIC.
After thawing, DIN samples were analysed by automated colorimetric techniques (San++ SKALAR). DIC analysis was performed using a segmented flow analyser (San++ SKALAR) according to the method of Stoll et al. (2001). DIC and nutrient fluxes were calculated from the linear change in concentration in the overlying water between T_{end} and T_1, standardized for overlying water volume and fluid exchange surface, and correcting for concentration changes due to the water replacement.

2.2.2.3. Irrigation tracer.
Bromide anions (in 2016) were separated by ion chromatography (Dionex Ionpac AS14 column), using a 3.5 mM Na$_2$CO$_3$/1 mM NaHCO$_3$ eluent. They were then detected by an UV spectrophotometer (Thermo Ultimate-3000) and an electrochemical detector (Dionex ED40). Uranine samples (in 2017) were analysed using a spectrophotometer ($\lambda_{excitation}$ = 494 μm, $\lambda_{emission}$ = 515 μm).

The irrigation rate Q (L d^{-1}) (Meysman et al., 2006) was estimated as

$$Q = -\frac{V_{OW}}{(Cr_0 - Cr_{reference})} \cdot \frac{dC}{dt} \tag{2}$$

with V_{OW} the volume of overlying water, C_{T0} the tracer concentration at the beginning of the incubation, $C_{T\ reference}$ the ambient tracer concentration of seawater, and dC/dt the slope of the decreasing tracer concentration over time. The slope between T_0 and T_1 was selected since this represents best the actual irrigation rate rather than the depth of the irrigation (De Borger et al., 2020). The irrigation rates were standardized by dividing Q by the surface of the core (L m^{-2} d^{-1}).

2.2.3. Biological samples

The benthic organisms were identified to the lowest possible taxonomic level, typically to species level, counted, and the blotted wet weight determined. The abundance and biomass data, standardized to m^2, were used to calculate two functional indices of the benthic community: the bioturbation potential (BP$_c$, Eq. (3)) (Solan et al., 2004) and the irrigation potential (IP$_c$, Eq. (4)) (Wrede et al., 2018). For each species i in a sample, the abundance and biomass (resp. A_i and B_i) were scaled, and multiplied with either its mobility score M_i and reworking score R_i (for the BP$_c$; Queirós et al., 2013), or its burrow type BT_i, feeding type FT_i, and injection pocket depth ID_i (for IP$_c$; Wrede et al., 2018).

$$BP_C = \sum_{i=1}^{n} \left(\frac{B_i}{A_i}\right)^{0.5} \cdot A_i \cdot M_i \cdot R_i \tag{3}$$

$$IP_C = \sum_{i=1}^{n} \left(\frac{B_i}{A_i}\right)^{0.75} \cdot A_i \cdot BT_i \cdot FT_i \cdot ID_i \tag{4}$$

2.3. Mass balance modelling

Biogeochemical process rates were estimated based on measured fluxes of O$_2$, DIC, NH$_x$ and NO$_x$ and an integrated mass balance of oxygen, carbon, nitrate and ammonium in the sediment, which is an extension of the model developed in Soetaert et al. (2001). This model contains the following processes: organic carbon can be oxidized aerobically (oxic mineralization - OxicMin), anaerobically (anoxic mineralization – AnoxicMin) or by denitrification (Denitr). Anoxic mineralization in this model consists of the collected anoxic mineralization sub-processes (e.g. Mn and Fe reduction, and methanogenesis, as per Soetaert et al. (1996)). Reduced substances, also called Oxygen Demanding Units (ODU), produced by anoxic mineralization can be deposited in the sediment and remain buried (ODUdeposition), or be re-oxidized (Reoxidation – Reoxi). Oxygen can be used to oxidize organic carbon (OxicMin), to re-oxidize ODU (Reoxi) and to oxidize ammonium to nitrate (Nitrification – Nitr) which requires two moles of oxygen for each mole of ammonium (Eq. (5)). On the other hand, dissolved inorganic carbon (DIC) is produced by organic carbon mineralization (OxicMin, AnoxicMin, Denitr) (Eq. (6)). Ammonium is produced by the mineralization of organic nitrogen (Total N mineralization - Nmin) and the dissimilatory nitrate reduction to ammonium (DNRA), while it is consumed by nitrification (Eq. (7)). Nitrate is produced by nitrification and consumed by denitrification (0.8 mol of NO$_3$/mol of carbon denitrified) and DNRA (Eq. (8)). Oxygen, DIC, nitrate, and ammonium are further exchanged through the sediment-water interface (O2influx, CO2efflux, NOxinflux, NHxinflux), while the lower boundary of the sediment is assumed to be a no flux boundary. The resulting balances are summarized below.

$$\frac{dO_2}{dt} = O_2 influx - OxicMin - Reoxidation - Nitrification*2 \tag{5}$$

$$\frac{dCO_2}{dt} = CO_2 efflux - OxicMin - AnoxicMin - Denitrification \tag{6}$$

$$\frac{dNH_x}{dt} = NH_x influx + Nmineralization + DNRA - Nitrification \tag{7}$$

$$\frac{dNO_x}{dt} = NO_x influx + Nitrification - 0.8*Denitrification - DNRA \tag{8}$$

The fluxes across the sediment-water interface (O_2 influx, CO_2 efflux, NH_x influx, NO_x influx) were estimated during the incubation experiments, while the rates of change of oxygen, carbon dioxide, nitrate and ammonium fluxes were assumed to be zero (geochemical steady state). Two extra equations were added to solved the unmeasured quantities (OxicMin, AnoxicMin, ODUdeposition, Reoxi, Nmin, Nitr, Denitr, DNRA): the reoxidation of reduced substances equals the anoxic mineralization minus the ODU that remains buried (Eq. (9)), and the total N mineralization equals the sum of all mineralization processes (OxicMin, AnoxicMin, Denitr) with a relationship between nitrogen and carbon mineralization using the Redfield N/C ratio (0.156) (Eq. (10)).

$$Reoxi = AnoxicMin - ODUdeposition \qquad (9)$$

$$
\begin{aligned}
&Nmineralisation \\
&= (OxicMin + AnoxicMin + Denitrification) * N/C\ ratio \qquad (10)
\end{aligned}
$$

All unknowns should be equal to or above 0. The mass balance model is based on two assumptions: the system reached a geochemical steady state and there was no carbonate dissolution or formation.

With 6 equations and 8 unknowns, the model was underdetermined and the R package limSolve (Soetaert et al., 2009) was used to solve a Least Squares with Equality and Inequality Constraints inverse problem (lsei, type 2).

2.4. Statistical analysis

2.4.1. Multiple factor analysis

To visualize common patterns between the environmental parameters, species composition and biogeochemical characteristics, a Multiple Factor Analysis (MFA) was applied (Escofier and Pagès, 1994). MFA is a multivariate analysis performed in two steps: in a first step, principle component analyses (PCA) on separate tables of variables (environment, fauna, biogeochemistry) are performed, and the components of the PCA's are then normalized by dividing all elements by the total inertia obtained from the respective PCAs. In the second step the weighted PCA tables are combined and again subjected to PCA to generate the reference structure; the common structure of all the data. For the initial PCA's in step one, environmental parameters (permeability, sediment granulometry, TOC, TOM, chl a) and biogeochemical parameters (process rates modelled in Section 2.4) were subjected to correlation matrix PCA; species biomass was log-transformed and subjected to a centred PCA (Dray and Dufour, 2007).

2.4.2. Variance partitioning

Variance partitioning was used to determine which biogeochemical processes are predominantly influenced by the sediment variables or by faunal components. This technique allows parts of the explained variance of a response variable to be attributed to individual subsets of potentially correlated explanatory variables (Borcard et al., 2011). In this case, the explanatory variables combined all environmental variables as one subset (Table 1), and the biological variables as the other (Table 2); the response variables were the modelled biogeochemical process rates. Since variance partitioning is based on linear relationships, linearity between the sets of the explanatory variables and each individual response variable was assessed through linear regression testing, assuming a p-value of 0.05 for significance. Explanatory variables (and in one case the response variable) were square root, or log transformed to resolve issues of non-linearity. If linearity could not be achieved, the variable was left out of the subset entirely (modelled variable and removed variables were for Oxic min: TOM, TOC, irrigation rate; for Anoxic min.: fines, all species variables; for Denitr: fines, vfines, BP_c, IP_c, species richness; for Nmin: fines, vfines; for Nitr: TOC, TOM, permeability, porosity, MGS, silt; SCOC: irrigation rate, species richness). Explanatory variables were centred on their means and standardized to control for the different scales of the response variables in the subsets (Legendre and Legendre, 1998). A forward selection procedure was applied on the subsets of explanatory variables to remove redundancy (Blanchet et al., 2008). After the variance partitioning, the significance of each partition of explained variance was assessed using a permutation test, assuming a p-value of 0.05 (Borcard et al., 2011).

2.4.3. Statistical modelling

To statistically correlate SCOC, estimated oxic and anoxic mineralization, denitrification, nitrification and total N mineralization to environmental and biological explanatory variables, a multiple linear regression approach was used. Prior to the model construction, collinear predictors were excluded from the full set of predictors until all the variance inflation factor (VIF) values were lower than 5 (Zuur et al., 2007). The full linear models included permeability, % of Total Organic Matter (TOM), % of fines (125–250 μm), BP_c, IP_c, irrigation rate and species richness as predictors. Model selection was performed through a stepwise procedure based on the Akaike Information Criterium (AIC). After selection of the best model, the assumptions were checked with graphical techniques. No violation of the assumptions was noticed for the SCOC and denitrification models. However, heterogeneity of variance in the residuals was detected for the other models. Linear regression with a generalized least-squares extension was then performed for the oxic, anoxic and total mineralization models (Chapter 4 in Zuur et al., 2009). The variance structure used for each model is summarized in Table 4. To model nitrification, a generalized linear model (GLM) with a gamma distribution was adopted as this response variable is continuous and larger than zero. Finally, the relative consumption of nitrate by denitrification (denitrification / (denitrification + DNRA)) was modelled using a GLM with a quasibinomial distribution.

Data analysis and modelling was performed in R (R Core Team, 2020), using the software packages "ade4" for the MFA (Dray and

Table 1
Sediment characteristics. Values are expressed as average ± sd ($n = 3$).

Year	Station	Permeability 10^{-12} m^2	MGS μm	Silt %	Fine sand %	Very fine sand %	Porosity -	TOC %	TOM %	Chl a μg g^{-1}
2016	130	$1.98\ 10^{-3} \pm 0.12\ 10^{-3}$	14 ± 1	87 ± 8	6 ± 6	4 ± 1	0.77 ± 0.02	1.67 ± 0.22	8.81 ± 0.94	95 ± 33.8
	780	0.18 ± 0.03	176 ± 1	12 ± 0	66 ± 3	9 ± 0	0.49 ± 0.05	0.23 ± 0.05	1.14 ± 0.34	3.2 ± 0.9
	BRN11	10.2 ± 0.45	294 ± 6	0 ± 0	31 ± 2	0 ± 0	0.41 ± 0.08	0.07 ± 0.01	0.52 ± 0.01	0.3 ± 0.1
	330	14.4 ± 0.79	349 ± 10	0 ± 0	15 ± 2	0 ± 0	0.35 ± 0.09	0.1 ± 0	0.55 ± 0.01	0.1 ± 0
	BBEG	41.10 ± 3.75	574 ± 32	0 ± 0	0 ± 0	0 ± 0	0.22 ± 0.14	0.03 ± 0.01	0.32 ± 0.1	0.1 ± 0
2017	130	0.12 ± 0.13	19 ± 2	75 ± 5	14 ± 4	5 ± 1	0.75 ± 0.03	0.74 ± 0.25	5.4 ± 2.39	31.5 ± 10
	780	0.37 ± 0.32	169 ± 3	19 ± 2	58 ± 2	9 ± 1	0.51 ± 0.05	0.24 ± 0.06	1.58 ± 0.23	9.6 ± 0.4
	120	5.29 ± 4.12	221 ± 9	9 ± 5	47 ± 8	5 ± 3	0.42 ± 0.03	0.13 ± 0.04	1.07 ± 0.18	2.7 ± 0.3
	BRN11	13.1 ± 4.25	253 ± 6	3 ± 3	45 ± 0	1 ± 0	0.39 ± 0.02	0.09 ± 0.03	0.73 ± 0.01	0.9 ± 0.2
	D6N	18.7 ± 7.00	353 ± 12	0 ± 0	16 ± 4	0 ± 0	0.36 ± 0.02	0.07 ± 0.01	0.43 ± 0.04	0.2 ± 0.1
	330	42.5 ± 1.83	434 ± 43	0 ± 0	5 ± 4	0 ± 0	0.33 ± 0.01	0.06 ± 0.01	0.82 ± 0.1	0.2 ± 0
	D6S	53.9 ± 19.7	524 ± 203	0 ± 0	5 ± 5	0 ± 0	0.35 ± 0.1	0.04 ± 0.01	0.91 ± 0.37	0.1 ± 0

Table 2
Variables used for describing the biological functioning in the different stations, for successive years. Values are expressed as average $\pm$ sd, for three replicates (n = 3).

Year	Station	Irrigation rate L m^{-2} d^{-1}	IP$_c$ gWW$^{0.75}$ m^{-2}	BP$_c$ gWW$^{0.5}$ m^{-2}	Abundance Ind. m^{-2}	Biomass gWW m^{-2}
2016	130	3.31 $\pm$ 2.79	125 $\pm$ 130	212 $\pm$ 186	297 $\pm$ 194	10 $\pm$ 11
	780	1.17 $\pm$ 0.09	6014 $\pm$ 1981	4017 $\pm$ 1190	1443 $\pm$ 482	1035 $\pm$ 130
	BRN11	24.92	112 $\pm$ 81	269 $\pm$ 78	270 $\pm$ 178	6 $\pm$ 2
	330	2.12 $\pm$ 0.8	282 $\pm$ 132	390 $\pm$ 110	788 $\pm$ 489	9 $\pm$ 7
	BBEG	6.7 $\pm$ 3.21	5 $\pm$ 6	21 $\pm$ 25	24 $\pm$ 20	1 $\pm$ 1
2017	130	15.64 $\pm$ 2.31	2341 $\pm$ 1845	2834 $\pm$ 1678	2716 $\pm$ 2617	387 $\pm$ 267
	780	6.42 $\pm$ 0.82	4106 $\pm$ 2381	6299 $\pm$ 2891	6196 $\pm$ 3184	772 $\pm$ 440
	120	0.62 $\pm$ 0.65	1340 $\pm$ 1279	2021 $\pm$ 1192	4923 $\pm$ 701	451 $\pm$ 593
	BRN11	7.76 $\pm$ 0.33	2760 $\pm$ 3980	1294 $\pm$ 689	811 $\pm$ 106	157 $\pm$ 207
	D6N	4.98 $\pm$ 2.08	715 $\pm$ 547	831 $\pm$ 205	1317 $\pm$ 283	23 $\pm$ 14
	330	10.91 $\pm$ 8.93	24 $\pm$ 12	163 $\pm$ 119	200 $\pm$ 81	2 $\pm$ 1
	D6S	3.95 $\pm$ 1.04	40 $\pm$ 55	175 $\pm$ 215	435 $\pm$ 181	3 $\pm$ 5

Dufour, 2007), the "vegan" package for the variance partitioning (Oksanen et al., 2019), the "limSolve" package for the mass balance model (van den Meersche et al., 2009) and the "lmne" (Pinheiro et al., 2020) and "MASS" (Ripley et al., 2020) packages for the linear models.

3. Results

3.1. Field measurements

3.1.1. Sediment

Sediments ranged from silty sediments with a high total organic matter (TOM) content and a low permeability nearshore (st. 130: median grain size (MGS) = 19 $\pm$ 2 μm, TOM = 5.4 $\pm$ 2.4%, permeability = 0.12 10^{-12} $\pm$ 0.13 10^{-12} m^2, values as average $\pm$ sd), to highly permeable, coarse grained sediments with lower total organic matter contents further offshore (D6S: MGS = 524 $\pm$ 203 μm, TOM = 0.91 $\pm$ 0.37%, permeability = 53.9 10^{-12} $\pm$ 19.7 10^{-12} m^2) (Table 1, Fig. 2A). Stations BRN11, 120, and 780 represented fine sandy sediments of intermediate grain size (169 $\pm$ 3–253 $\pm$ 6 μm), characterized by a high percentage of fine sands (45 $\pm$ 0–58 $\pm$ 2%), low to intermediate permeability (0.18 10^{-12} $\pm$ 0.03 10^{-12}–13.10 10^{-12} $\pm$ 4.25 10^{-12} m^2), and a TOM content varying from 0.52 $\pm$ 0.01% to 1.58 $\pm$ 0.23%. Sediments were classified as permeable (D6, BBEG, BRN11, 330), or cohesive (120, 130, 780), depending on whether their permeability was above (permeable), or below (cohesive) 2.5*10^{-12} m^2 (Forster et al., 2003; Wilson et al., 2008).

3.1.2. Fauna

Species abundance and biomass were highest in the cohesive sediments (sts. 120, 130, 780) in both years, with up to 6196 $\pm$ 3184 ind. m^{-2} representing 772 $\pm$ 440 g WW m^{-2} at st. 780 (Table 2). The
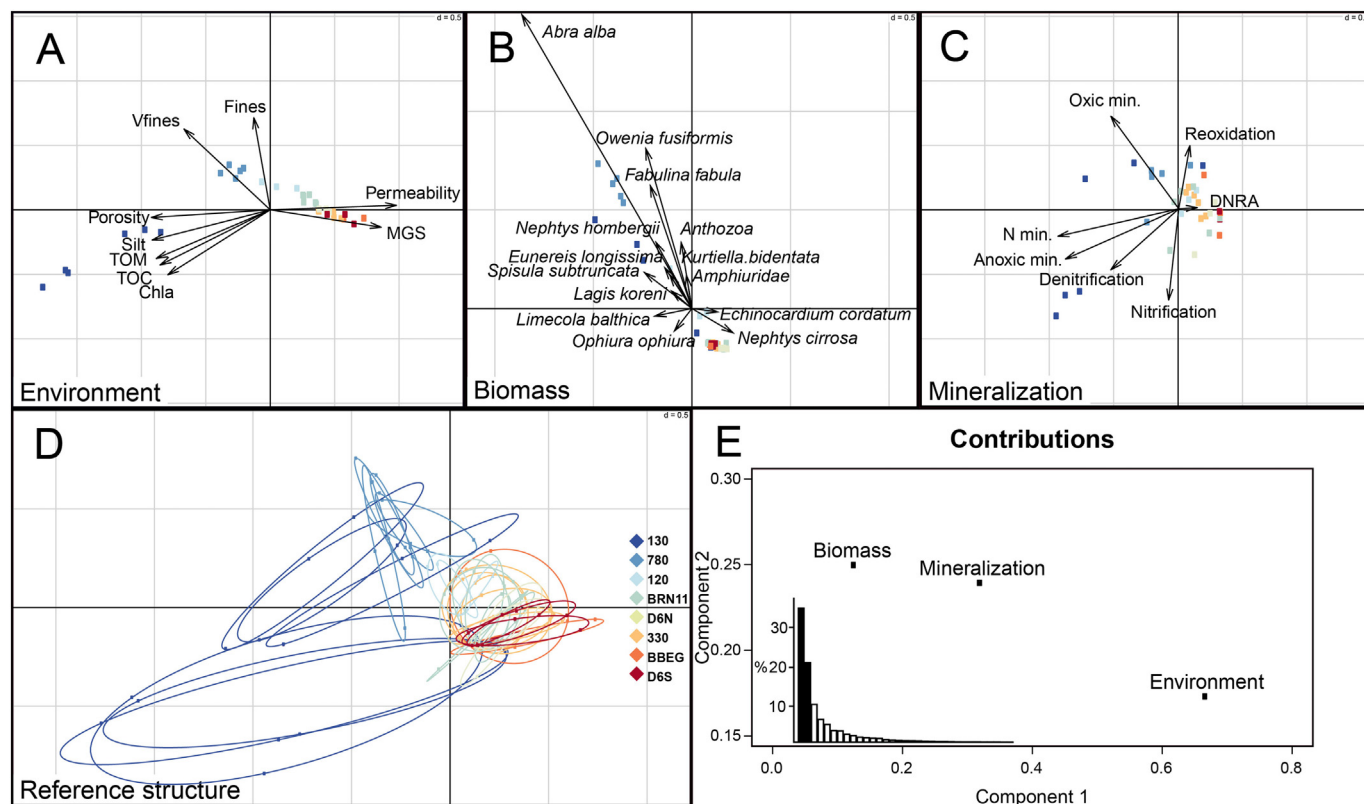

Fig. 2. Multiple factor analysis (MFA). A–C: Ordination of the samples based on sediment parameters (A), species biomass (B), and modelled process rates (C). D: Position of the samples for all parameter tables grouped per set of samples. An ellipse represents one set of samples. Ellipses are a graphical summary of the means (the reference structure), variances and the covariance of the three coordinates of the sample. Panels A–D share their coordinate system and are directionally compatible for interpretation. E: Relative influence of each table (red text) to first and second MFA components (axes); the histogram shows the relative importance of the first and second axes (black) relative to additional axes. (For interpretation of the references to colour in this figure legend, the reader is referred to the web version of this article.)

species communities in sts. 120 and 780 were representative of the *Abra alba* community (Breine et al., 2018; Van Hoey et al., 2004), with the bivalve *Abra alba* present in nearly every sample in combination with other bivalve species such as *Kurtiella bidentata*, *Fabulina fabula*, and the tube building polychaete *Owenia fusiformis* (Fig. 2B). Station 130, in turn, was representative of the *Limecola balthica* community (Degraer et al., 2003). In the permeable sediments (sts. 330, D6, BBEG, BRN11) values for the species metrics were lower, with abundances and biomasses between 24 ± 20 and 1317 ± 283 ind. m^{-2}, and between 1 ± 1 and 157 ± 207 g WW m^{-2} respectively. As a result, values of the functional indices BP_c (21 ± 25–1294 ± 689 gWW$^{0.5}$ m^{-2}) and IP_c (5 ± 5–2760 ± 3980 gWW$^{0.75}$ m^{-2}) were low in the permeable sediments (with the exception of BRN11 in 2017 (IP_c: 2760 ± 3980 gWW$^{0.75}$ m^{-2}, BP_c: 1294 ± 689 gWW$^{0.5}$ m^{-2}), and high in the cohesive sediments (BP_c: 212 ± 186–6299 ± 2891 gWW$^{0.5}$ m^{-2}; IP_c: 125 ± 130–6014 ± 1981 gWW$^{0.75}$ m^{-2}, Table 2). Species in the permeable sediments generally belonged to the *Nephtys cirrosa* community (Van Hoey et al., 2004), with *Nephtys cirrosa* dominating the biomass in every sample except for the BBEG samples (Fig. 2B). The amphipod species *Urothoe brevicornis* and *U. poseidonis* were present in all samples besides the BBEG and D6S samples. The amphipod species *Bathyporeia elegans* and *B. guilliamsoniana* were also absent from the latter samples, as well as from st. 330 in 2017. Macrofauna communities at D6S were poor in species, in contrast to D6N, where additional species such as the sea urchin *Echinocardium cordatum*, the hermit crab species *Diogenes pugilator*, and the polychaete species *Eteone* sp. and *Spiophanes bombyx* were recorded.

3.1.3. Fluxes and mineralization processes

The total modelled C mineralization decreased with the permeability gradient, ranging from 168 ± 74 mmol C m^{-2} d^{-1} in muddy sediment (st. 130) to 0.21 ± 0.19 mmol C m^{-2} d^{-1} in the coarsest and most permeable sediment (st. D6S) (Fig. 3A). The same pattern was observed for the estimated anoxic mineralization that exhibited large and strongly variable rates in muddy sediments (St. 130, 135 ± 75 mmol C

m^{-2} d^{-1}) and extremely low rates in coarse sediment from station D6S (0.1 ± 0.1 mmol C m^{-2} d^{-1}) (Fig. 3D, Appendix B in supplementary material).

The measured SCOC and the estimated oxic mineralization rates were higher in all sediments with low permeability (Fig. 3B & C). The SCOC showed the highest rates in the fine sandy station 780 in both years (SCOC: 48.7 ± 2.2 mmol O_2 m^{-2} d^{-1} in 2016, 57.3 ± 15.1 mmol O_2 m^{-2} d^{-1} in 2017) while the oxic mineralization showed the highest rates at 780 in 2016 (35.2 ± 7.5 mmol C m^{-2} d^{-1}) and at the muddy station 130 in 2017 (43.1 ± 19.3 mmol C m^{-2} d^{-1}) (Appendix B in supplementary material).

No clear pattern along the permeability gradient was found for estimated denitrification, nitrification nor for DNRA (Fig. 4). In general, denitrification rates ranged between 0 ± 0 and 14.3 ± 2.6 mmol N m^{-2} d^{-1}, indicating almost no denitrification in the coarsest sediments from stations D6N and BBEG (0 ± 0–0.4 ± 0.6 mmol C m^{-2} d^{-1}). Nitrification and DNRA rates revealed high interannual variation, especially at the muddy station 130, where both the lowest modelled rates (Nitr: 1.3 ± 2.2 N m^{-2} d^{-1} in 2017, DNRA: 0 ± 0 N m^{-2} d^{-1} in 2016) and the highest modelled rates (Nitr: 15.3 ± 2.4 mmol N m^{-2} d^{-1} in 2016, DNRA: 12.3 ± 7 N m^{-2} d^{-1} in 2017) were estimated (Appendix B in supplementary material).

The first two components of the MFA explained 60% of the variance in the combined dataset (Fig. 2D, E). The sediment variables were the dominant contributor to the first component, followed by the mineralization processes, and the species community matrix (Fig. 2E). The second component was mostly related to the community structure in terms of species biomass and the mineralization processes, with a lower contribution of the sediment variables.

3.2. Variance partitioning

Variance partitioning indicated that the biological component ([bio] column, Table 3) was a significant explanatory variable of the oxic mineralization, denitrification and SCOC. The sediment subset ([sed]
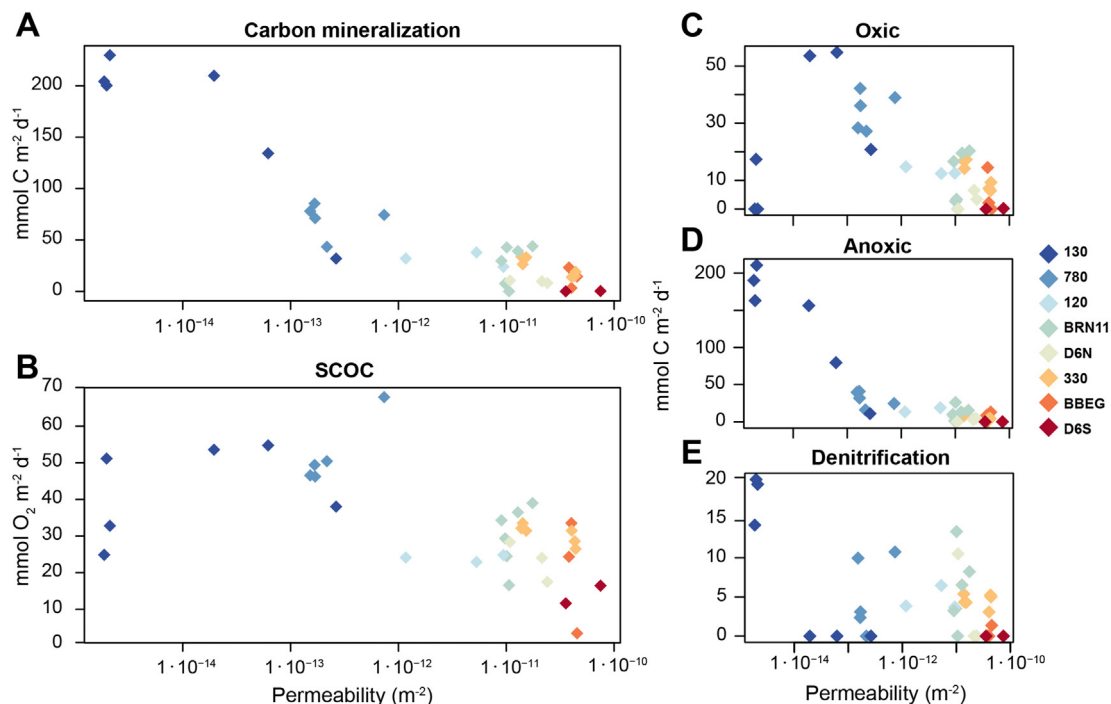

Fig. 3. Carbon mineralization processes: (A) Total organic carbon mineralization (mmol C m^{-2} d^{-1}); (B) Sediment community oxygen consumption (mmol O_2 m^{-2} d^{-1}); (C)– (E) Rate of carbon mineralization allocated to oxic or anoxic mineralization, or denitrification (mmol C m^{-2} d^{-1}). Values represented as a function of log transformed permeability (x-axis). Permeability gradient indicated by different colours (For interpretation of the references to colour in this figure legend, the reader is referred to the web version of this article.).
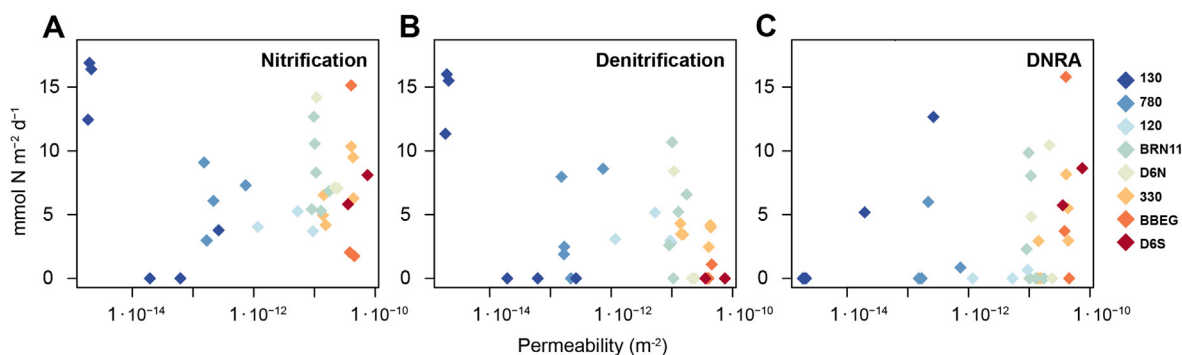
Fig. 4. Nitrogen cycling processes: (A) Nitrification; (B) Denitrification; (C) Dissimilatory nitrate reduction to ammonium (DNRA). Values as mmol N m^{-2} d^{-1} and represented as a function of log transformed permeability (x-axis).

column, Table 3) was significant in explaining the estimated anoxic mineralization, denitrification, and the (log transformed) N mineralization. Except for denitrification, a substantial part (6–49%) of variance was explained by both the biology and the sediment as shared variance([co] column, Table 3). The forward selection procedure did not select any significant explanatory variables from the biological component for anoxic mineralization. Similarly, none of the sediment-related components were selected as a significant explanatory variable for nitrification. In these instances, the variable with the highest significance was chosen to run the analysis with (Table 3). As a result, the model for anoxic mineralization was fully composed of the sediment parameters while the model for nitrification only comprised the species component (Table 3).

3.3. Statistical modelling

The results of the statistical models confirm that the sediment variables were particularly important in explaining anoxic processes while biological variables were particularly important in the models for oxic processes (Table 4). Anoxic mineralization increased with TOM content while it decreased with permeability. TOM and fines were positively related to denitrification. Our models show that an increased irrigation rate had a negative effect on denitrification and anoxic mineralization and on the probability of nitrate to be consumed by denitrification rather than by DNRA.

The sediment reworking activity of the macrobenthos, estimated by BP$_c$, enhanced all three modelled oxic processes: SCOC, oxic mineralization and nitrification. The SCOC was also negatively correlated to the permeability.

Finally, the variance in total N mineralization was explained both by sediment variables (permeability and TOM) and by biological variables (BP$_c$ and irrigation rate).

4. Discussion

4.1. Spatial patterns

Our results indicated a clear link between the sedimentary environment, the sediment-inhabiting fauna and the estimated biogeochemical rates. All these properties varied substantially within the study area, notably changing along a gradient from cohesive sediments with high mineralization rates (sts. 120, 130, 780), to permeable sediments with low mineralization rates (D6, BBEG, 330, Fig. 2).

The reported oxygen consumption rates (14–57 mmol O$_2$ m^{-2} d^{-1}), nitrification (1–15 mmol N m^{-2} d^{-1}), and denitrification (0–14 mmol N m^{-2} d^{-1}) were generally in line with those found previously in the area (Braeckman et al., 2014) and other coastal North Sea stations (Lohse et al., 1993; Marchant et al., 2016; Bratek et al., 2020). Nitrification and denitrification rates reported from the German Bight, a nearby coastal environment characterized by a high deposition rate, were also in line with the values obtained during the present study (Neumann et al., 2017).

The high estimated total mineralization rates in cohesive sediments (31–213 mmol C m^{-2} d^{-1}) were not matched by similar oxygen consumption rates (Fig. 3A-B). Especially in St. 130, DIC fluxes were exceptionally high, opening up the possibility that the steady state assumption for the mass balance model was not met for these samples, given these high fluxes could result from increased respiration

Table 3
Results of the variance partitioning procedure for the two methodologies: use of stepwise variable selection from the subset of variables selected through variance inflation testing (VIF), and the stepwise variable selection from all variables (All). [bio] and [sed] are the conditional effects of the species component and the sediment component respectively, [co] represents the jointly explained variance, and [res] the residuals of the full model [bio + co + sed]. Numbers show the adjusted R^2 for the model fractions and are in bold when significant as determined by the permutation test.

	Variables	[bio + co]	[co + sed]	[bio + co + sed]	[bio]	[co]	[sed]	[res]
SCOC	[bio] √BP$_c$	**0.50**	**0.34**	**0.53**	**0.19**	0.31	0.03	0.47
	[sed] Permeability, fine							
Oxic mineralization	[bio] BP$_c$, species richness	**0.64**	**0.30**	**0.64**	**0.33**	0.30	**0**	0.36
	[sed] Permeability, fine							
Anoxic mineralization	[bio] √SpRichness*	0.06	**0.89**	**0.90**	0.0	0.05	**0.84**	0.1
	[sed] Perm., TOM, Fine							
Nitrification	[bio] IP$_c$	**0.15**	0.04	**0.12**	0.08	0.06	0	0.88
	[sed] fine*							
Denitrification	[bio] IrrigationRate	0.07	**0.24**	**0.32**	**0.07**	0	**0.25**	0.68
	[sed] permeability							
Log N mineralization	[bio] √BP$_c$	0.13	**0.73**	**0.72**	0	0.13	**0.60**	0.28
	[sed] permeability							

* Denotes variables that were not statistically significant ($p < 0.05$) according to the forward selection procedure but were most significant out of the set of variables.

Table 4

Summary of the significant (p < 0.05) predictive models for SCOC, oxic mineralization, anoxic mineralization, total N mineralization, nitrification and the probability of nitrate being transformed into nitrogen gas through denitrification. For each model, the distribution and the variance structure when applicable are detailed. The AIC and the adjusted R-squared or explained deviance when available are provided, when available.

Model formula	Distribution	Variance structure	AIC
$\text{SCOC} = 32.73^{***} - 2.23\ 10^{11}\ \text{Permeability}^{*} + 5.41\ 10^{-3}\ \text{BP}_c^{***} - 0.59\ \text{SpeciesRichness}$	Gaussian (LM)		AIC = 160 Adj R^2 = 58%
$\text{Oxic mineralization} = 11.09^{***} + 6.91\ 10^{-3}\ \text{BP}_c^{***} - 1.29\ 10^{11}\ \text{Permeability} - 0.42\ \text{SpeciesRichness}$	Gaussian (GLS)	Power of variance covariate ~ Permeability	AIC = 276
$\text{Anoxic mineralization} = 7.72^{***} - 3.37\ 10^{11}\ \text{Permeability}^{***} + 14.64\ \text{TOM}^{***} - 0.16\ \text{IrrigationRate}^{***}$	Gaussian (GLS)	Exponential of variance covariate ~ TOM	Station	AIC = 265
$\text{N mineralization} = 3.96^{***} - 7.66\ 10^{10}\ \text{Permeability}^{***} + 3.01\ \text{TOM}^{***} + 8.25\ 10^{-4}\ \text{BP}_c^{*} - 7.89\ 10^{-2}\ \text{IrrigationRate}^{*}$	Gaussian (GLS)	Different standard deviation ~ Station	AIC = 214
$\text{Nitrification} = 0.11^{***} + 3.13\ 10^{-5}\ \text{BP}_c^{*}$	Gamma (GLM)		AIC = 210 Explained Deviance = 6%
$\text{Denitrification} = 2.71 + 1.40\ \text{TOM}^{***} + 0.10\ \text{Fines}^{*} - 0.27\ \text{IrrigationRate}^{*} - 1.09\ 10^{-3}\ \text{IP}_c^{*}$	Gaussian (LM)		AIC = 105 Adj R^2 = 46%
$\text{Den / Den + DNRA} = 1.21^{*} - 0.17\ \text{IrrigationRate}^{*}$	Binomial (GLM)		AIC = 46 Explained Deviance = 16%

* P < 0.05.
*** P < 0.001.

stimulated by high temperatures during transport. The steady-state assumption does not imply that nothing is changing in the sediment at all, but that changes in time of solid and liquid constituents (nutrient fluxes, the porewater concentrations, and solid substances in the sediment) are much smaller than the process rates themselves, so that they can be ignored. Given the otherwise acceptable agreement between the SCOC and DIC fluxes, and time elapsed since the peak organic matter deposition, we expect this assumption to have been fulfilled in the other stations. In permeable sediments on the other hand, often more oxygen was consumed (13–32 mmol $O_2\ m^{-2}\ d^{-1}$) than needed for mineralization alone (0.2–31 mmol C $m^{-2}\ d^{-1}$), with a larger allocation of the SCOC to nitrification, and the reoxidation of reduced products of anoxic mineralization.

We observed a shift from denitrification to DNRA as the main NO_3^- consuming process (up to 100%) towards more irrigated sediments (Table 4). This is consistent with previous studies, where maximal rates for DNRA in permeable sediments were 50% and 77% of the total NO_3^- consumption based on field cores (Hellemann et al., 2020) and slurry experiments (Behrendt et al., 2013) respectively. DNRA is performed by many anaerobic prokaryotes, but has been shown to occur in eukaryotes as well (Kamp et al., 2015). In permeable sands, advective flows can rapidly transport algal cells such as diatoms deep in the sediments (Huettel and Rusch, 2000), where temporary anoxia or dark conditions, along with sufficient concentrations of NO_3^- could induce nitrate reduction by diatoms, to survive dark conditions (Kamp et al., 2011). With denitrification strongly dependent on the organic matter content of the sediment (Table 4), our observations suggest that DNRA increases in importance relative to denitrification when high nitrate concentrations are available (e.g. by ventilation activity, which favours both DNRA and denitrification), but where concentrations of organic matter to mineralize are lower (disfavouring denitrification, since this is strictly heterotrophic).

Alternatively, it is possible that the increasing irrigation rate promotes nitrogen fixation by bringing N_2 rich water deeper in the sediment. Nitrogen fixation transforms N_2 into NH_4^+ and appears to be more important than previously believed in marine sediments (Bertics et al., 2010; Newell et al., 2016). Fan et al. (2015) showed that N_2 fixation occurs in Southern North Sea sediments, and exhibits similar rates as denitrification, with highest N_2 fixation rates observed in permeable sediments. N_2 fixed in the sediment would end up in both measurable NH_4^+ effluxes from the sediment and in biomass (and through biomass degradation to NH_4^+ concentrations) (Newell et al., 2016). Hence, part of the NH_4^+ production in the model may be due to N_2 fixation, and part of the NO_3^- consumption by denitrification, as opposed to DNRA. However, additional measurements (e.g. of the N_2 flux), would have been needed to constrain the N_2 fixation process in the mass balance model. As is, the inclusion of DNRA, and the differentiation between oxic and anoxic mineralization are already useful improvements over previous applications of the mass balance approach (Soetaert et al., 1996; Braeckman et al., 2010, 2014). Given that only a few studies exist which describe DNRA, nitrogen fixation and anammox (anoxic ammonium oxidation) for the southern North Sea (e.g. Bale et al., 2014; Fan et al., 2015; Lipsewers et al., 2014), it would be of high interest to perform dedicated microbial and ^{15}N stable isotope research, to better understand the abiotic and biotic factors regulating the relative occurrence of these N-cycling processes in temperate coastal areas.

4.2. Respective roles of macrobenthos and sediment characteristics in C and N cycling

Variance partitioning and multiple linear regression both showed that oxic processes were mainly related to faunal activities, whereas anoxic processes were more determined by sediment characteristics. Denitrification was significantly linked to both components. Moreover, the interaction between faunal and abiotic components was of primordial importance for all modelled processes except denitrification.

4.2.1. Faunal activities play a major role in C and N cycling

The key role that macrobenthos activity plays in benthic mineralization processes is well described (e.g. Braeckman et al., 2014; Kristensen, 2001; Volkenborn et al., 2016). In our study, we used the Bioturbation Potential (BP_c) and the Irrigation Potential (IP_c) of the community as proxies for two types of faunal activity, respectively particle reworking and burrow ventilation. Variance partitioning showed that BP_c explained a considerable amount of variance in oxic processes, and BP_c was selected in regression models for SCOC, oxic mineralization, total N mineralization, and nitrification (Table 4). Particle reworking enhances SCOC, by mixing buried reduced compounds back into the oxic zone of the sediment, where they are reoxidized (Aller, 1978). At the same time, bioturbators fragment organic matter and disperse it from the sediment-water interface where it originally settled, to a larger volume of sediment. This makes it more accessible to micro-organisms, and results in increased mineralization rates, both oxic and anoxic (van Nugteren et al., 2009; Canfield et al., 1993; Canfield and Thamdrup, 1994).

While burrow ventilation fuels oxic mineralization and nitrification by bringing electron acceptors (e.g. O_2, NO_3^-) deeper in the sediment (Aller and Aller, 1998; Banta et al., 1999), the IP_c index was *not* selected as an explanatory variable, despite previous findings that stressed the importance of burrow ventilation (Mermillod-Blondin et al., 2004; Braeckman et al., 2010; Wrede et al., 2018). We suspect this could be due to different reasons. First, the IP_c index might not be an accurate estimation of the burrow ventilation rate. De Borger et al. (2020) indeed showed that IP_c correlates more strongly to the burrow ventilation depth than to the ventilation rate and our results do not indicate any correlation between the IP_c index and the measured irrigation rate (Appendix C in supplementary material). Second, BP_c and IP_c represent faunal activities that affect sediments at different timescales. Both functional indices represent the *potential* to express an activity, but they do not include the temporal dynamics of the activity. Temporal variation is strongly pronounced for ventilation as animals do not ventilate constantly (Volkenborn et al., 2016), and the downward transported electron acceptors (e.g. oxygen) are rapidly consumed. As such, the stimulation of oxic mineralization processes takes place at short temporal scales, which is not taken into account in the IP_c formulation. Temporal dynamics are less pronounced for particle transport. Though organisms do not move constantly either, bioturbation displaces particulate organic matter to deeper layers, where it is mineralized over a much longer timeframe relative to the quasi-instantaneous consumption of oxygen, thus generating a longer lasting effect. We believe that IP_c could be more useful in predicting biogeochemical processes if a metric for temporal dynamics were included in the index.

Our results do not support the common idea that ventilation increases rates of coupled nitrification-denitrification (Pelegri et al., 1994; Rysgaard et al., 1995; Na et al., 2008; Volkenborn et al., 2016). Indeed, nitrification rates were strongly and positively related to faunal activities, but denitrification rates were negatively correlated to the irrigation rate and to IP_c (Table 4). Irrigation brings both nitrate and oxygen in the pore water at depth. Nitrification is then enhanced as oxygen serves as an electron acceptor but the high oxygen concentration or the low OM availability might inhibit denitrification (Bergaust et al., 2012). Similar patterns have been observed before. For example, *Trypaea australiensis* (a marine ghost shrimp) which constructs deep burrow systems and exhibits high particle transport and ventilation rates has been shown to stimulate nitrification, without affecting rates of denitrification. This uncoupling of nitrification and denitrification was probably due to larger spatial separation between nitrification and denitrification zones (Jordan et al., 2009).

Unlike denitrification, the importance of DNRA increased in well-irrigated sediments (Model of Denitrification / (Denitrification + DNRA), Table 4) which results in the retention of reactive nitrogen in the marine environment. It is unclear why the ventilation rate would influence the balance between DNRA and denitrification in this way. We speculate that DNRA is more efficient to deal with oxic conditions than denitrification. Indeed, Roberts et al. (2014) showed that the contribution of DNRA to nitrate reduction increased from <1% in anoxic conditions to 18% in oxic conditions.

4.2.2. Permeability, an important environmental variable for total C and N cycling

At first sight, the high importance of permeability in our study is in contrast with the well-established idea that fauna plays an important role in the benthic biogeochemistry. Other studies using variance partitioning techniques have reported a more balanced importance of biotic and abiotic variables in ecosystem functioning (Belley and Snelgrove, 2016; Godbold and Solan, 2009). However, these studies focused on a narrow part of the permeability gradient (MGS 20–112 µm), where faunal activities play a more important role in mineralization processes than in truly permeable sediment (Braeckman et al., 2014). The importance of permeability in explaining biogeochemical processes in permeable sediments has been highlighted before (Huettel et al.,

2014), but our study is the first to show the importance of permeability for total carbon and nitrogen mineralization along such a wide gradient of permeability.

Permeability alone explained 60% of the variability in total N mineralization (Table 4). The oxic part of mineralization was mainly related to faunal activities, but the variability in anoxic mineralization and denitrification, which together account for more than half of the total mineralization in most stations, was mainly explained by sediment characteristics (respectively 84% and 25%), with permeability as the main selected variable (Table 3, Table 4). Permeability is a key factor for ecosystem functioning as it affects oxygen and food availability in the sediment, but it is also a structuring factor of the habitats and microbial communities (Seitzinger et al., 2006; Probandt et al., 2017). Indeed, sediments characterized by low permeability, high percentage of TOM and a high percentage of fine sands (125–250 µm) create a favourable environment for denitrifiers and in particular sulphate reducers (Seitzinger et al., 2006; Al-Raei et al., 2009; Probandt et al., 2017).

In addition to permeability, the total organic matter content was an important environmental variable for the estimations of anoxic mineralization, denitrification and total N mineralization (Table 4). This is not unexpected, since a higher OM content will trigger higher mineralization rates (Al-Raei et al., 2009), hence lead to oxygen depletion. Despite similar bottom water chl *a* concentrations in the study area at the end of summer (Braeckman et al., 2014), the OM content tends to be lower in coarse permeable sediment, which probably indicates that most of the OM is already recycled at the end of summer in those highly active sediments (Huettel et al., 2003; Rasheed et al., 2003). Therefore, it would be interesting to investigate the relationship between permeability and mineralization processes in different seasons, to be able to determine the impact of permeability throughout the year.

4.2.3. Sediment – fauna interactions

The sediment properties and the inhabiting benthic fauna are closely related, as variance partitioning showed considerable covariance between both in the models for SCOC, oxic mineralization, and total N mineralization (Table 3). This is in line with results of other studies using variance partitioning (Godbold and Solan, 2009; Belley and Snelgrove, 2016), where shared variability between biotic and abiotic factors remained present as a predictor for benthic biogeochemistry.

Benthic communities are strongly associated to certain ranges of sediment characteristics, such as median grain size, and the mud content, which are linked to water column processes that govern food availability and hydrodynamic stress (e.g. Llobet-Brossa et al., 1998, 2002; Degraer et al., 1999; Böttcher et al., 2000; Van Hoey et al., 2004; Al-Raei et al., 2009; Vanaverbeke et al., 2011). Moreover, different sediment types impose different constraints on the fauna, resulting in a variable expression of effect traits along a range of habitats. We found high values for both BP_c and IP_c in fine sandy – muddy sediments, and lowest values in the most permeable, coarse sediments (Table 1, Table 2). Braeckman et al. (2014) similarly demonstrated that BP_c was a major predictor of SCOC and NH_x exchange in fine sandy sediments, and to a lesser extent in muddy and permeable sediments. While the higher values of the functional indices in finer sediment are partly attributed to higher faunal biomass, the functional traits of only few species in permeable sediments (e.g. the sea urchins *Echinocardium* sp. and the polychaetes *Nephtys* sp., Appendix D in supplementary material) attain high values which contribute markedly to the index scores.

In permeable sediments, macrofauna tend to have response traits that make them more adapted to stronger hydrodynamic pressures, while they are less constrained by low oxygen availability than species in cohesive sediments (Vanaverbeke et al., 2011). Whereas ventilation rates were of similar magnitude in permeable and cohesive sediments (Table 2), our measurements do not separate faunal burrow ventilation from physical ventilation. In permeable sediments, local hydrodynamics induce advective porewater flows that overwhelm animal pumping activities (Kristensen and Kostka, 2013;

Huettel et al., 2014). It is thus difficult to provide statements about the actual ventilation rates in permeable sediments, based on organism trait scores alone. In cohesive sediments however, solute exchange with the overlying water is limited to the scale of a few millimetres by diffusive transport, which makes burrow ventilation and particle transport interesting processes from the organismal point of view to replenish oxygen and food supply, and remove metabolites (Aller and Aller, 1998; Meysman et al., 2006; Volkenborn et al., 2016).

As such, our results show the usefulness of using effect traits as predictors for ecosystem processes, but similarly highlight the caveat of interpreting them when calculated without proper consideration of environmental steering. This again shows that the use of functional trait indices is likely of little use without associated investigation of metrics of ecosystem functionality (Bolam and Eggleton, 2014).

4.3. Models to understand the impact of anthropogenic activities on mineralization processes

Three of the studied stations were more strongly impacted by human activities. Station BRN11 is located in an abandoned sand extraction area, and stations D6N and D6S are situated 200 m north and south from an offshore wind turbine (Fig. 1). In this section, we discuss how environmental changes triggered by anthropogenic activities impact estimated mineralization rates and how the models that we applied could be a useful tool to understand those impacts.

We observed that stations experiencing anthropogenic impact were highly variable in time (BRN11) and in space (D6N & D6S). Compared to the situation in 2016, sediment from BRN11 in 2017 had higher fine sand and silt fractions, lower permeability and higher chl *a* content (Table 1). In addition, the macrobenthic community was much more diverse; and associated BP_c and IP_c were higher (Table 2). The irrigation rates were quite similar. Comparable differences were observed between D6N (finer sediment, richer in chl *a* and fauna) and D6S, although only 400 m apart.

The reasons for the observed sedimentary and biological changes are unclear. At BRN11, the temporal changes following the closure of the site could be attributed to ongoing sand extraction activity in the vicinity, to the migration of sand dunes, or a combination of both, that contribute to fining of the sediment in the extraction pit (Degrendele and Vandenreyken, 2017; De Backer, pers. obs.). The spatial differences observed around wind turbine D6 could be due to altered local hydrodynamics linked to the presence of the turbine (Rivier et al., 2016; Legrand et al., 2018) or to the position on the sand wave (Cheng et al., 2020), in combination with the deposition of (pseudo)faeces by filter feeders living abundantly on the turbine (Coates et al., 2013; Baeye and Fettweis, 2015).

Regardless of the exact causes, these results tend to suggest that sediment fining causes a shift in the macrobenthos community, and enhances the estimated mineralization processes, as shown by higher oxic and anoxic mineralization rates in the finer-grained stations (Appendix B in supplementary material). Our regression models (Table 4) have proven to be useful in understanding these impacts. For instance, the increased potential of the community to rework particles along with the lower permeability in the finer-grained stations explain their enhanced oxic mineralization rates (Oxic mineralization model, Table 4).

The models developed here are a major step forward towards predicting and scaling up the effects of anthropogenic activities on different ecosystem functions in shallow North Sea sediments, which is crucial to support scientifically sound ecosystem management.

5. Conclusions

In this study, we disentangled biotic and abiotic driving forces of benthic biogeochemical processes by applying variance partitioning on biogeochemical rates obtained via a mass balance model. While oxic processes were mainly regulated by faunal activities and advective processes in permeable sediments, anoxic mineralization was controlled by sediment characteristics. However, for processes such as denitrification, the sediment and its inhabiting fauna were too strongly linked to be separated. As a result, we showed that organism traits are useful to predict biogeochemical processes but should be interpreted in the right ecological context. Regression models were derived to estimate biogeochemical processes as a function of biotic and abiotic variables. They may prove to be a useful tool to understand the impact of anthropogenic activities and provide a step towards predicting and scaling up their impact on ecosystem functions.

CRediT authorship contribution statement

Elise Toussaint: Conceptualization, Methodology, Formal analysis, Investigation, Data curation, Writing - original draft, Visualization. **Emil De Borger:** Conceptualization, Methodology, Formal analysis, Investigation, Writing - original draft, Visualization. **Ulrike Braeckman:** Conceptualization, Methodology, Writing - review & editing, Funding acquisition. **Annelies De Backer:** Writing - review & editing. **Karline Soetaert:** Methodology, Writing - review & editing, Funding acquisition. **Jan Vanaverbeke:** Conceptualization, Formal analysis, Writing - review & editing, Supervision, Project administration, Funding acquisition.

Declaration of competing interest

The authors declare that they have no known competing financial interests or personal relationships that could have appeared to influence the work reported in this paper.

Appendix A. Supplementary data

Supplementary data to this article can be found online at https://doi.org/10.1016/j.scitotenv.2021.144994.

References

Aller, R.C., 1978. In: Wiley, M.L. (Ed.), The Effects of Animal-Sediment Interactions on Geochemical Processes near the Sediment-Water Interface. Estuarine Interactions, Academic Press, pp. 157–172 https://doi.org/10.1016/B978-0-12-751850-3.50017-0.

Aller, R.C., 1980. Quantifying solute distributions in the bioturbated zone of marine sediments by defining an average microenvironment. Geochim. Cosmochim. Acta 44, 1955–1965. https://doi.org/10.1016/0016-7037(80)90195-7.

Aller, R.C., Aller, J.Y., 1992. Meiofauna and solute transport in marine muds. Limnol. Oceanogr. 37, 1018–1033. https://doi.org/10.4319/lo.1992.37.5.1018.

Aller, R.C., Aller, J.Y., 1998. The effect of biogenic irrigation intensity and solute exchange on diagenetic reaction rates in marine sediments. J. Mar. Res. 56, 905–936. https://doi.org/10.1357/002224098321667413.

Aller, R.C., Yingst, J.Y., 1985. Effects of the marine deposit-feeders Heteromastus filiformis (Polychaeta), Macoma balthica (Bivalvia), and Tellina texana (Bivalvia) on averaged sedimentary solute transport, reaction rates, and microbial distributions. J. Mar. Res. 43, 615–645. https://doi.org/10.1357/002224085788440349.

Al-Raei, A.M., Bosselmann, K., Böttcher, M.E., Hespenheide, B., Tauber, F., 2009. Seasonal dynamics of microbial sulfate reduction in temperate intertidal surface sediments:

controls by temperature and organic matter. Ocean Dyn. 59, 351–370. https://doi.org/10.1007/s10236-009-0186-5.

Baeye, M., Fettweis, M., 2015. In situ observations of suspended particulate matter plumes at an offshore wind farm, southern North Sea. Geo-Marine Lett. 35, 247–255. https://doi.org/10.1007/s00367-015-0404-8.

Bale, N.J., Villanueva, L., Fan, H., Stal, L.J., Hopmans, E.C., Schouten, S., Sinninghe Damst, J.S., 2014. Occurrence and Activity of Anammox Bacteria in Surface Sediments of the Southern North Sea. https://doi.org/10.1111/1574-6941.12338.

Banta, G.T., Holmer, M., Jensen, M.H., Kristensen, E., 1999. Effects of two polychaete worms, Nereis diversicolor and Arenicola marina, on aerobic and anaerobic decomposition in a sandy marine sediment. Aquat. Microb. Ecol. 19, 189–204. https://doi.org/10.3354/ame019189.

Behrendt, A., De Beer, D., Stief, P., 2013. Vertical activity distribution of dissimilatory nitrate reduction in coastal marine sediments. Biogeosciences 10, 7509–7523. https://doi.org/10.5194/bg-10-7509-2013.

Belley, R., Snelgrove, P.V.R., 2016. Relative contributions of biodiversity and environment to benthic ecosystem functioning. Front. Mar. Sci. 3, 242. https://doi.org/10.3389/fmars.2016.00242.

Bergaust, L., van Spanning, R.J.M., Frostegård, Å., Bakken, L.R., 2012. Expression of nitrous oxide reductase in Paracoccus denitrificans is regulated by oxygen and nitric oxide through FnrP and NNR. Microbiology 158, 826–834. https://doi.org/10.1099/mic.0.054148-0.

Bertics, V., Sohm, J., Treude, T., Chow, C., Capone, D., Fuhrman, J., Ziebis, W., 2010. Burrowing deeper into benthic nitrogen cycling: the impact of bioturbation on nitrogen fixation coupled to sulfate reduction. Mar. Ecol. Prog. Ser. 409, 1–15. https://doi.org/10.3354/meps08639.

Blanchet, F.G., Legendre, P., Borcard, D., 2008. Forward selection of explanatory variables. Ecology 89, 2623–2632. https://doi.org/10.1890/07-0986.1.

Bolam, S.G., Eggleton, J.D., 2014. Macrofaunal production and biological traits: spatial relationships along the UK continental shelf. J. Sea Res. 88, 47–58. https://doi.org/10.1016/j.seares.2014.01.001.

Borcard, D., Gillet, F., Legendre, P., 2011. Numerical Ecology with R, Numerical Ecology with R. https://doi.org/10.1007/978-1-4419-7976-6.

Böttcher, M.E., Hespenheide, B., Llobet-Brossa, E., Beardsley, C., Larsen, O., Schramm, A., et al., 2000. The biogeochemistry, stable isotope geochemistry, and microbial community structure of a temperate intertidal mudflat: an integrated study. Cont. Shelf Res. 20, 1749–1769. https://doi.org/10.1016/S0278-4343(00)00046-7.

Braeckman, U., Provoost, P., Gribsholt, B., Van Gansbeke, D., Middelburg, J.J., Soetaert, K., Vincx, M., Vanaverbeke, J., 2010. Role of macrofauna functional traits and density in biogeochemical fluxes and bioturbation. Mar. Ecol. Prog. Ser. 399, 173–186. https://doi.org/10.3354/meps08336.

Braeckman, U., Foshtomi, M.Y., Van Gansbeke, D., Meysman, F., Soetaert, K., Vincx, M., Vanaverbeke, J., 2014. Variable importance of macrofaunal functional biodiversity for biogeochemical cycling in temperate coastal sediments. Ecosystems 17, 720–737. https://doi.org/10.1007/s10021-014-9755-7.

Bratek, A., Van Beusekom, J.E.E., Neumann, A., Sanders, T., Friedrich, J., et al., 2020. Spatial variations in sedimentary N-transformation rates in the North Sea (German Bight). Biogeosciences 17, 2839–2851. https://doi.org/10.5194/bg-17-2839-2020.

Breine, N.T., De Backer, A., Van Colen, C., Moens, T., Hostens, K., Van Hoey, G., 2018. Structural and functional diversity of soft-bottom macrobenthic communities in the southern North Sea. Estuar. Coast. Shelf Sci. 214, 173–184. https://doi.org/10.1016/j.ecss.2018.09.012.

Bremner, J., Rogers, S., Frid, C., 2003. Assessing functional diversity in marine benthic ecosystems: a comparison of approaches. Mar. Ecol. Prog. Ser. 254, 11–25. https://doi.org/10.3354/meps254011.

Buchanan, J.B., 1984. In: Holmes, N.A., McIntyre, A.D. (Eds.), Sediment Analysis, 2nd ed. Blackwell Scientific Publications, Oxford https://doi.org/10.1002/9781118542392.

Canfield, D.E., Thamdrup, B., 1994. The production of 34S-depleted sulfide during bacterial disproportionation of elemental sulfur. 266. American Association for the Advancement of Science, pp. 1973–1975. https://doi.org/10.1126/science.11540246.

Canfield, D., Jørgensen, B., Fossing, H., Glud, R., Gundersen, J., Ramsing, N., et al., 1993. Pathways of organic carbon oxidation in three continental margin sediments. Mar. Geol. 113, 27–40. https://doi.org/10.1016/0025-3227(93)90147-N.

Cheng, C.H., Soetaert, K., Borsje, B.W., 2020. Sediment characteristics over asymmetrical tidal sand waves in the Dutch north sea. J. Mar. Sci. Eng. 8, 409. https://doi.org/10.3390/JMSE8060409.

Coates, D.A., Deschutter, Y., Vincx, M., Vanaverbeke, J., 2013. Enrichment and shifts in macrobenthic assemblages in an offshore wind farm area in the Belgian part of the North Sea wind farm area in the Belgian part of the North Sea. Mar. Environ. Res., 1–12 https://doi.org/10.1016/j.marenvres.2013.12.008.

Coates, D.A., Deschutter, Y., Vincx, M., Vanaverbeke, J., 2014. Enrichment and shifts in macrobenthic assemblages in an offshore wind farm area in the Belgian part of the North Sea. Mar. Environ. Res. 95, 1–12. https://doi.org/10.1016/j.marenvres.2013.12.008.

De Beer, D., Wenzhöfer, F., Ferdelman, T.G., Boehme, S.E., Huettel, M., Van Beusekom, J.E.E., et al., 2005. Transport and mineralization rates in North Sea sandy intertidal sediments, Sylt-Rømø Basin, Wadden Sea. Limnol. Oceanogr. 50, 113–127. https://doi.org/10.4319/lo.2005.50.1.0113.

De Borger, E., Tiano, J., Braeckman, U., Ysebaert, T., Soetaert, K., 2020. Biological and biogeochemical methods for estimating bio-irrigation: a case study in the Oosterschelde estuary. Biogeosciences 17, 1701–1715. https://doi.org/10.5194/bg-2019-413.

De Smet, B., Braeckman, U., Soetaert, K., Vincx, M., Vanaverbeke, J., 2016. Predator effects on the feeding and bioirrigation activity of ecosystem-engineered Lanice conchilega reefs. J. Exp. Mar. Biol. Ecol. 475, 31–37. https://doi.org/10.1016/j.jembe.2015.11.005.

Degraer, S., Meire, P., Vincx, M., Meire+, P., Offringa+, H., 1999. The macrozoobenthos of an important wintering area of the common scoter (Melanitta nigra). J. Mar. Biol. Assoc. UK 79, 243–251. https://doi.org/10.1017/S0025315498000277.

Degraer, S., Van Lancker, V., Moerkerke, G., Van Hoey, G., Vanstaen, K., Vincx, M., Henriet, J.-P., 2003. Evaluation of the ecological value of the foreshore: habitat-model and macrobenthic side-scan sonar interpretation: extension along the Belgian Coastal Zone. Final report. Ministry of the Flemish Community, Environment and Infrastructure Department. Waterways and Marine Affairs Administration, Coastal Waterways, p. 63.

Degraer, S., Verfaillie, E., Willems, W., Adriaens, E., Vincx, M., Van Lancker, V., 2008. Habitat suitability modelling as a mapping tool for macrobenthic communities: an example from the Belgian part of the North Sea. Cont. Shelf Res. 28, 369–379. https://doi.org/10.1016/j.csr.2007.09.001.

Degrendele, K., Vandenreyken, H., 2017. Belgian Marine Sand: A Scarce Resource?

Díaz, S., Cabido, M., 2001. Vive la différence: plant functional diversity matters to ecosystem processes. Trends Ecol. Evol. 16, 646–655. https://doi.org/10.1016/S0169-5347(01)02283-2.

Dray, S., Dufour, A.-B., 2007. The ade4 package: implementing the duality diagram for ecologists. J. Stat. Softw. 22, 1–20. https://doi.org/10.18637/jss.v022.i04.

Duncan, C., Thompson, J.R., Pettorelli, N., 2015. The quest for a mechanistic understanding of biodiversity–ecosystem services relationships. Proc. R. Soc. B Biol. Sci. 282. https://doi.org/10.1098/rspb.2015.1348.

Eggleston, J., Rojstaczer, S., 1998. Inferring spatial correlation of hydraulic conductivity from sediment cores and outcrops. Geophys. Res. Lett. 25, 2321–2324. https://doi.org/10.1029/98GL01773.

Ehrenhauss, S., Witte, U., Janssen, F., Huettel, M., 2004. Decomposition of diatoms and nutrient dynamics in permeable North Sea sediments. Cont. Shelf Res. 24, 721–737. https://doi.org/10.1016/j.csr.2004.01.002.

Eigaard, O.R., Bastardie, F., Hintzen, N.T., Buhl-Mortensen, L., Buhl-Mortensen, P., Catarino, R., Dinesen, G.E., Egekvist, J., Fock, H.O., Geitner, K., Gerritsen, H.D., González, M.M., Jonsson, P., Kavadas, S., Laffargue, P., Lundy, M., Gonzalez-Mirelis, G., Nielsen, J.R., Papadopoulou, N., Posen, P.E., Pulcinella, J., Russo, T., Sala, A., Silva, C., Smith, C.J., Vanelslander, B., Rijnsdorp, A.D., 2017. The footprint of bottom trawling in European waters: distribution, intensity, and seabed integrity. ICES J. Mar. Sci. 74, 847–865. https://doi.org/10.1093/icesjms/fsw194.

Escofier, B., Pagès, J., 1994. Multiple factor analysis (AFMULT package). Comput. Stat. Data Anal. 18, 121–140. https://doi.org/10.1016/0167-9473(94)90135-X.

Fan, H., Bolhuis, H., Stal, L.J., 2015. Drivers of the dynamics of diazotrophs and denitrifiers in North Sea bottom waters and sediments. Front. Microbiol. 6, 738. https://doi.org/10.3389/fmicb.2015.00738.

Fettweis, M., Houziaux, J.S., Du Four, I., Van Lancker, V., Baeteman, C., Mathys, M., Van den Eynde, D., Francken, F., Wartel, S., 2009. Long-term influence of maritime access works on the distribution of cohesive sediments: analysis of historical and recent data from the Belgian nearshore area (southern North Sea). Geo-Marine Lett. 29, 321–330. https://doi.org/10.1007/s00367-009-0161-7.

Forster, S., Bobertz, B., Bohling, B., 2003. Permeability of sands in the coastal areas of the southern Baltic Sea: mapping a grain-size related sediment property. Aquat. Geochem. 9, 171–190. https://doi.org/10.1023/B:AQUA.0000022953.52275.8b.

Froelich, P.N., Klinkhammer, G.P., Bender, M.L., Luedtke, N.A., Heath, G.R., Cullen, D., Dauphin, P., Hammond, D., Hartman, B., Maynard, V., 1979. Early oxidation of organic matter in pelagic sediments of the eastern equatorial Atlantic: suboxic diagenesis. Geochim. Cosmochim. Acta 43, 1075–1090. https://doi.org/10.1016/0016-7037(79)90095-4.

Gaston, G.R., Bartlett, J.H.W., Mcallister, A.P., Heard, R.W., 1996. Biomass variations of estuarine macrobenthos preserved in ethanol and formalin. Estuaries 19, 674–679. https://doi.org/10.2307/1352527.

GEBCO Compilation Group, 2020. GEBCO 2020 Grid [WWW Document]. https://doi.org/10.5285/a29c5465-b138-234d-e053-6c86abc040b9.

Glud, R.N., Forster, S., Huettel, M., 1996. Influence of Radial Pressure Gradients on Solute Exchange in Stirred Benthic Chambers.

Godbold, J.A., Solan, M., 2009. Relative importance of biodiversity and the abiotic environment in mediating an ecosystem process. Mar. Ecol. Prog. Ser. 396, 273–282. https://doi.org/10.3354/meps08401.

Gogina, M., Lipka, M., Woelfel, J., Liu, B., Morys, C., Böttcher, M.E., et al., 2018. In search of a field-based relationship between benthic macrofauna and biogeochemistry in a modern brackish coastal sea. Front. Mar. Sci. 5, 1–18. https://doi.org/10.3389/fmars.2018.00489.

Gust, G., Harrison, J.T., 1981. Biological pumps at the sediment-water interface: mechanistic evaluation of the alpheid shrimp Alpheus mackayi and its irrigation pattern. Mar. Biol. 64, 71–78. https://doi.org/10.1007/BF00394082.

Hellemann, D., Tallberg, P., Aalto, S., Bartoli, M., Hietanen, S., 2020. Seasonal cycle of benthic denitrification and DNRA in the aphotic coastal zone, northern Baltic Sea. Mar. Ecol. Prog. Ser. 637, 15–28. https://doi.org/10.3354/meps13259.

Hillman, J.R., Stephenson, F., Thrush, S.F., Lundquist, C.J., 2020. Investigating changes in estuarine ecosystem functioning under future scenarios. Ecol. Appl. 30. https://doi.org/10.1002/eap.2090.

Huettel, M., Gust, G., 1992. Impact of bioroughness on interfacial solute exchange in permeable sediments. Mar. Ecol. Prog. Ser. 89, 253–267. https://doi.org/10.3354/meps089253.

Huettel, M., Rusch, A., 2000. Transport and degradation of phytoplankton in permeable sediment. Limnol. Oceanogr. 45, 534–549. https://doi.org/10.4319/lo.2000.45.3.0534.

Huettel, M., Røy, H., Precht, E., Ehrenhauss, S., 2003. Hydrodynamical impact on biogeochemical processes in aquatic sediments. Hydrobiologia 494, 231–236.

Huettel, M., Berg, P., Kostka, J.E., 2014. Benthic exchange and biogeochemical cycling in permeable sediments. Annu. Rev. Mar. Sci. 6, 23–51. https://doi.org/10.1146/annurev-marine-051413-012706.

Jordan, M.A., Welsh, D.T., Dunn, R.J.K., Teasdale, P.R., 2009. Influence of Trypaea australiensis population density on benthic metabolism and nitrogen dynamics in sandy estuarine sediment: a mesocosm simulation. J. Sea Res. 61, 144–152. https://doi.org/10.1016/j.seares.2008.11.003.

Jørgensen, B.B., 2000. Bacteria and Marine Biogeochemistry. Marine Geochemistry. Berlin/Heidelberg: Springer-Verlag, pp. 169–206 https://doi.org/10.1007/3-540-32144-6_5.

Jørgensen, B.B., Glud, R.N., Holby, O., 2005. Oxygen Distribution and Bioirrigation in Arctic Fjord Sediments (Svalbard, Barents Sea). 292 pp. 85–95.

Kamp, A., De Beer, D., Nitsch, J.L., Lavik, G., Stief, P., 2011. Diatoms respire nitrate to survive dark and anoxic conditions. Proc. Natl. Acad. Sci. U. S. A. 108, 5649–5654. https://doi.org/10.1073/pnas.1015744108.

Kamp, A., Høgslund, S., Risgaard-Petersen, N., Stief, P., 2015. Nitrate storage and dissimilatory nitrate reduction by eukaryotic microbes. Front. Microbiol. 6. https://doi.org/10.3389/fmicb.2015.01492.

Kristensen, E., 2001. Impact of polychaetes (Nereis spp. and Arenicola marina) on carbon biogeochemistry in coastal marine sediments. Geochem. Trans. 2, 92–103. https://doi.org/10.1039/b108114d.

Kristensen, E., Kostka, J.E., 2013. Macrofaunal burrows and irrigation in marine sediment: microbiological and biogeochemical interactions. Interact. Between Macro- Microorg. Mar. Sediments, 125–157 https://doi.org/10.1029/CE060p0125.

Kristensen, E., Penha-Lopes, G., Delefosse, M., Valdemarsen, T., Quintana, C.O., Banta, G.T., 2012. What is bioturbation? The need for a precise definition for fauna in aquatic sciences. Mar. Ecol. Prog. Ser. 446, 285–302. https://doi.org/10.3354/meps09506.

Lavorel, S., Garnier, E., 2002. Predicting changes in community composition and ecosystem functioning from plant traits: revisiting the holy grail. Funct. Ecol. https://doi.org/10.1046/j.1365-2435.2002.00664.x.

Legendre, P., Legendre, L.F.J., 1998. Numerical ecology. Developments in Environmental Modelling, 2nd ed Elsevier Science, Amsterdam.

Legrand, S., de la Vallée, P., Fettweis, M., Van Den Eynde, D., 2018. Permanente en significante wijzigingen van de hydrografische eigenschappen, Belgische staat, 2018: Atcualisatie van de initiële beoordeling voor de Belgische mariene wateren. Kaderrichtlijn Mariene Strategie – Art 8 lid 1a & 1b. België, Brussel.

Lipsewers, Y.A., Bale, N.J., Hopmans, E.C., Schouten, S., Sinninghe Damsté, J.S., Villanueva, L., 2014. Seasonality and depth distribution of the abundance and activity of ammonia oxidizing microorganisms in marine coastal sediments (North Sea). Front. Microbiol. 5, 472. https://doi.org/10.3389/fmicb.2014.00472.

Llobet-Brossa, E., Rosselló-Mora, R., Amann, R., 1998. Microbial community composition of Wadden Sea sediments as revealed by fluorescence in situ hybridization. Appl. Environ. Microbiol. 64, 2691–2696. https://doi.org/10.1128/AEM.64.7.2691-2696.1998.

Llobet-Brossa, E., Rabus, R., Böttcher, M.E., Könneke, M., Finke, N., Schramm, A., et al., 2002. Community structure and activity of sulfate-reducing bacteria in an intertidal surface sediment: a multi-method approach. Aquat. Microb. Ecol. 29, 211–226. https://doi.org/10.3354/ame029211.

Lohse, L., Malschaert, J., Slomp, C., Helder, W., Van Raaphorst, W., 1993. Nitrogen cycling in North Sea sediments: interaction of denitrification and nitrification in offshore and coastal areas. Mar. Ecol. Prog. Ser. 101 (3), 283–296 Retrieved December 10, 2020, from. http://www.jstor.org/stable/24837975.

Marchant, H.K., Holtappels, M., Lavik, G., Ahmerkamp, S., Winter, C., Kuypers, M.M.M., 2016. Coupled nitrification-denitrification leads to extensive N loss in subtidal permeable sediments. Limnol. Oceanogr. 61, 1033–1048. https://doi.org/10.1002/lno.10271.

Matisoff, G., Fisher, J.B., Matis, S., 1985. Effects of benthic macroinvertebrates on the exchange of solutes between sediments and freshwater. Hydrobiologia 122, 19–33. https://doi.org/10.1007/BF00018956.

Mayer, L.M., 1994. Surface area control of organic carbon accumulation in continental shelf sediments. Geochim. Cosmochim. Acta 58, 1271–1284. https://doi.org/10.1016/0016-7037(94)90381-6.

McCave, I.N., Bryant, R.J., Cook, H.F., Coughanowr, C.A., 1986. Evaluation of a laser-diffraction-size analyzer for use with natural sediments. J. Sediment. Res. 56, 561–564. https://doi.org/10.1306/212f89cc-2b24-11d7-8648000102c1865d.

van den Meersche, K., Soetaert, K., van Oevelen, D., 2009. xsample: an R function for sampling linear inverse problems. J. Stat. Softw. 30. https://doi.org/10.1002/wics.10.

Mermillod-Blondin, F., Rosenberg, R., François-Carcaillet, F., Norling, K., Mauclaire, L., 2004. Influence of bioturbation by three benthic infaunal species on microbial communities and biogeochemical processes in marine sediment. Aquat. Microb. Ecol. 36, 271–284. https://doi.org/10.3354/ame036271.

Meysman, F.J.R., Galaktionov, O.S., Gribsholt, B., Middelburg, J.J., 2006. Bioirrigation in permeable sediments: Advective pore-water transport induced by burrow ventilation. Limnol. Oceanogr. 51, 142–156. https://doi.org/10.4319/lo.2006.51.1.0142.

MUMM Scientific Service, 2015. Sand and Gravel Extraction in the North Sea [WWW Document]. Manag. Mar. Environ.

Na, T., Gribsholt, B., Galaktionov, O., Lee, T., Meysman, F.J.R., 2008. Influence of advective bio-irrigation on carbon and nitrogen cycling in sandy sediments. J. Mar. Res. 66, 691–722.

Neumann, A., van Beusekom, J.E.E., Holtappels, M., Emeis, K.C., 2017. Nitrate consumption in sediments of the German bight (North Sea). J. Sea Res. 127, 26–35. https://doi.org/10.1016/j.seares.2017.06.012.

Newell, S.E., McCarthy, M.J., Gardner, W.S., Fulweiler, R.W., 2016. Sediment nitrogen fixation: a call for re-evaluating coastal N budgets. Estuar. Coasts 39, 1626–1638. https://doi.org/10.1007/s12237-016-0116-y.

Oksanen, J., Blanchet, F.G., Friendly, M., Kindt, R., Legendre, P., McGlinn, D., Minchin, P.R., O'Hara, R.B., Simpson, G.L., Solymos, P., Stevens, M.H.H., Szoecs, E., Wagner, H., 2019. vegan: Community Ecology Package.

Oldham, C., Ivey, G., Pullin, C., 2004. Estimation of a characteristic friction velocity in stirred benthic chambers. Mar. Ecol. Prog. Ser. 279, 291–295. https://doi.org/10.3354/meps279291.

Pelegri, S., Nielsen, L., Blackburn, T., 1994. Denitrification in estuarine sediment stimulated by the irrigation activity of the amphipod Corophium volutator. Mar. Ecol. Prog. Ser. 105, 285–290. https://doi.org/10.3354/meps105285.

Pinheiro, J., Bates, D., DebRoy, S., Sarkar, D., 2020. nlme: Linear and Nonlinear Mixed Effects Models.

Probandt, D., Knittel, K., Tegetmeyer, H.E., Ahmerkamp, S., Holtappels, M., Amann, R., 2017. Permeability shapes bacterial communities in sublittoral surface sediments. Environ. Microbiol. 19, 1584–1599. https://doi.org/10.1111/1462-2920.13676.

Provoost, P., Braeckman, U., Van Gansbeke, D., Moodley, L., Soetaert, K., Middelburg, J.J., Vanaverbeke, J., 2013. Modelling benthic oxygen consumption and benthic-pelagic coupling at a shallow station in the southern North Sea. Estuar. Coast. Shelf Sci. 120, 1–11. https://doi.org/10.1016/j.ecss.2013.01.008.

Queirós, A.M., Birchenough, S.N.R., Bremner, J., Godbold, J.A., Parker, R.E., Romero-Ramirez, A., Reiss, H., Solan, M., Somerfield, P.J., Van Colen, C., Van Hoey, G., Widdicombe, S., 2013. A bioturbation classification of European marine infaunal invertebrates. Ecol. Evol. 3, 3958–3985. https://doi.org/10.1002/ece3.769.

R Core Team, 2020. R: A Language and Environment for Statistical Computing.

Rasheed, M., Badran, M.I., Huettel, M., 2003. Influence of sediment permeability and mineral composition on organic matter degradation in three sediments from the Gulf of Aqaba. Red Sea. Estuar. Coast. Shelf Sci. 57, 369–384. https://doi.org/10.1016/S0272-7714(02)00362-1.

Ripley, B., Venables, B., Bates, D.M., Hornik, K., Gebhardt, A., Firth, D., 2020. Support Functions and Datasets for Venables and Ripley's MASS.

Rivier, A., Bennis, A.C., Pinon, G., Magar, V., Gross, M., 2016. Parameterization of wind turbine impacts on hydrodynamics and sediment transport. Ocean Dyn. 66, 1285–1299. https://doi.org/10.1007/s10236-016-0983-6.

Roberts, K.L., Kessler, A.J., Grace, M.R., Cook, P.L.M., 2014. Increased rates of dissimilatory nitrate reduction to ammonium (DNRA) under oxic conditions in a periodically hypoxic estuary. Geochim. Cosmochim. Acta 133, 313–324. https://doi.org/10.1016/j.gca.2014.02.042.

Rousseau, V., Lancelot, C., Cox, D., 2006. In: Rousseau, V., Lancelot, C., Brussels, D. Cox (Eds.), Current Status of Eutrophication in the Belgian Coastal Zone. Presse Universitaire de Bruxelles.

Rysgaard, S., Christensen, P.B., Nielsen, L.P., 1995. Seasonal variation in nitrification and denitrification in estuarine sediment colonized by benthic microalgae and bioturbation infauna. Mar. Ecol. Prog. Ser. 126, 111–121. https://doi.org/10.1007/BF01873045.

Seitzinger, S., Harrison, J.A., Böhlke, J.K., Bouwman, A.F., Lowrance, R., Peterson, B., Tobias, C., Van Drecht, G., 2006. Denitrification across landscapes and waterscapes: a synthesis. Ecol. Appl. 16, 2064–2090. https://doi.org/10.1890/1051-0761(2006)016[2064:DALAWA]2.0.CO;2.

Snelgrove, P., Butman, C.A., 1994. Animal-sediment relationships revisited: cause versus effect. Oceanogr. Mar. Biol. Annu. Rev. 32, 111–1777.

Snelgrove, P.V.R., Thrush, S.F., Wall, D.H., Norkko, A., 2014. Real world biodiversity-ecosystem functioning: a seafloor perspective. Trends Ecol. Evol. 29, 398–405. https://doi.org/10.1016/j.tree.2014.05.002.

Soetaert, K., Middelburg, J.J., 2009. Modeling eutrophication and oligotrophication of shallow-water marine systems: the importance of sediments under stratified and well-mixed conditions. Hydrobiologia 629, 239–254. https://doi.org/10.1007/s10750-009-9777-x.

Soetaert, K., Herman, P.M.J., Middelburg, J.J., 1996. A model of early diagenetic processes from the shelf to abyssal depths. Geochim. Cosmochim. Acta 60, 1019–1040. https://doi.org/10.1016/0016-7037(96)00013-0.

Soetaert, K., Herman, P.M., Middelburg, J.J., Heip, C., Smith, C.L., Tett, P., Wild-Allen, K., 2001. Numerical modelling of the shelf break ecosystem: reproducing benthic and pelagic measurements. Deep Sea Res. Part II Top. Stud. Oceanogr. 48, 3141–3177. https://doi.org/10.1016/S0967-0645(01)00035-2.

Soetaert, K., Van den Meersche, K., van Oevelen, D., 2009. limSolve: solving linear inverse models. R package 1.5.1.

Solan, M., Cardinale, B.J., Downing, A.L., Engelhardt, K.A.M., Ruesink, J.L., Srivastava, D.S., 2004. Extinction and ecosystem function in the marine benthos. Science (80-) 306, 1177–1180.

Stoll, M.H.C., Bakker, K., Nobbe, G.H., Haese, R.R., 2001. Continuous-flow analysis of dissolved inorganic carbon content in seawater. Anal. Chem. 73, 4111–4116. https://doi.org/10.1021/ac010303r.

Tous Rius, A., Denis, L., Dauvin, J.C., Spilmont, N., 2018. Macrobenthic diversity and sediment-water exchanges of oxygen and ammonium: example of two subtidal communities of the eastern English Channel. J. Sea Res. 136, 15–27. https://doi.org/10.1016/j.seares.2018.02.007.

Van Colen, C., Rossi, F., Montserrat, F., Andersson, M.G.I., Gribsholt, B., Herman, P.M.J., et al., 2012. Organism-sediment interactions govern post-hypoxia recovery of ecosystem functioning. PLoS One 7, e49795. https://doi.org/10.1371/journal.pone.0049795.

Van De Velde, S., Van Lancker, V., Hidalgo-Martinez, S., Berelson, W.M., Meysman, F.J.R., 2018. Anthropogenic disturbance keeps the coastal seafloor biogeochemistry in a transient state. Sci. Rep. 8. https://doi.org/10.1038/s41598-018-23925-y.

Van den Eynde, 2017. The Impact of Extraction on the Bottom Shear Stress Using the Proposed New Extraction Limit Levels. Royal Belgian Institute for Natural Sciences (ZAGRI-MOZ4-INDI67/1/DVDE/201706/EN/TR02).

Van Hoey, G., Degraer, S., Vincx, M., 2004. Macrobenthic community structure of soft-bottom sediments at the Belgian continental shelf. Estuar. Coast. Shelf Sci. 59, 599–613. https://doi.org/10.1016/j.ecss.2003.11.005.

van Nugteren, P., Moodley, L., Brummer, G.J., Heip, C.H.R., Herman, P.M.J., Middelburg, J.J., 2009. Seafloor ecosystem functioning: The importance of organic matter priming. Mar. Biol. 156, 2277–2287. https://doi.org/10.1007/s00227-009-1255-5.

Vanaverbeke, J., Merckx, B., Degraer, S., Vincx, M., 2011. Sediment-related distribution patterns of nematodes and macrofauna: two sides of the benthic coin? Mar. Environ. Res. 71, 31–40. https://doi.org/10.1016/j.marenvres.2010.09.006.

Violle, C., Navas, M.L., Vile, D., Kazakou, E., Fortunel, C., Hummel, I., Garnier, E., 2007. Let the concept of trait be functional! Oikos 116, 882–892. https://doi.org/10.1111/j.0030-1299.2007.15559.x.

Volkenborn, N., Woodin, S., Wethey, D., Polerecky, L., 2016. Bioirrigation in marine sediments. Reference Module in Earth Systems and Environmental Sciences. Elsevier Inc., pp. 1–9 https://doi.org/10.1016/B978-0-12-409548-9.09525-7.

Wentworth, C.K., 1922. A scale of grade and class terms for clastic sediments. J. Geol. 30, 377–392. www.jstor.org/stable/30063207.

Wetzel, M.A., Leuchs, H., Koop, J.H.E., 2005. Preservation effects on wet weight, dry weight, and ash-free dry weight biomass estimates of four common estuarine macro-invertebrates: no difference between ethanol and formalin. Helgol. Mar. Res. 59, 206–213. https://doi.org/10.1007/s10152-005-0220-z.

Wilson, A.M., Huettel, M., Klein, S., 2008. Grain size and depositional environment as predictors of permeability in coastal marine sands. Estuar. Coast. Shelf Sci. 80, 193–199. https://doi.org/10.1016/j.ecss.2008.06.011.

Wollast, R., 1998. "Evaluation and comparison of the global carbon cycle in the coastal zone and in the open ocean," in *The sea*. In: Brink, K.H., Robinson, A. (Eds.), John Wiley & Sons, Inc., Hoboken, New Jersey, pp. 213–252.

Wrede, A., Beermann, J., Dannheim, J., Gutow, L., Brey, T., 2018. Organism functional traits and ecosystem supporting services – a novel approach to predict bioirrigation. Ecol. Indic. 91, 737–743. https://doi.org/10.1016/J.ECOLIND.2018.04.026.

Wrede, A., Andresen, H., Asmus, R., Wiltshire, K.H., Brey, T., 2019. Macrofaunal irrigation traits enhance predictability of nutrient fluxes across the sediment-water interface. Mar. Ecol. Prog. Ser. 632, 27–42. https://doi.org/10.3354/meps13165.

Zuur, A.F., Ieno, E.N., Smith, G.M., 2007. Analysing Ecological Data. Springer, New-York.

Zuur, A.F., Ieno, E.N., Walker, N.J., Saveliev, A.A., Smith, G.M., 2009. Mixed Effects Models and Extensions in Ecology with R. Spr, New-York https://doi.org/10.4324/9780429201271-2.